Multiscale problems and their Asymptotic-Preserving resolution

Modeling, Simulation and Mathematical Analysis of Magnetically Confined Plasmas

Sinaia summer school 2019

French-Romanian Summer School on Applied Mathematics

Claudia NEGULESCU

UNIVERSITÉ Paul Sabatier, Toulouse III

Institut de Mathématiques de Toulouse

Mathématiques pour l'Industrie et la Physique

Unité Mixte de Recherches CNRS - Université Paul Sabatier Toulouse 3 - INSA Toulouse - Université Toulouse 1

UMR 5640

UFR MIG, Université Paul Sabatier Toulouse 3, 118 route de Narbonne, 31062 TOULOUSE cédex 4, France

Foreword

These lecture notes summarize a succession of works dealing with the construction as well as the mathematical and numerical study of Asymptotic-Preserving schemes for the resolution of multiscale problems in the kinetic framework. The lectures are based on articles, which were specifically chosen to illustrate different techniques in the design of AP-schemes and to treat different singular perturbation problems, occuring in the kinetic theory of thermonuclear fusion plasmas.
The goal of this notes is to familiarize the reader with the general features of AP-schemes, which can be further applied for singular perturbation problems arising in several other domains, as for example in the quatum mechanical framework.

This work has been carried out within the framework of the EUROfusion Consortium and has received funding from the Euratom research and training program 2014-2018 under grant agreement No 633053. The views and opinions expressed herein do not necessarily reflect those of the European Commission.

Table des matières

Introduction

The central theme of this course is the introduction and study of Asymptotic-Preserving schemes for the numerical simulation of singularly perturbed problems, arising in the description of systems composed of N charged particles, evolving in an electromagnetic field. The schemes presented here can be applied in various (other) physical contexts, as for example for neutral gases, quantum mechanical systems or other multiscale problems, however we shall focus in the present course on plasma physics.

The word "plasma" has been introduced for the first time by the Czech medical scientist Johannes Parkinje (1787-1869), to describe the blood, when cleared by its various corpuscles. It comes from the grec word $\pi\lambda\alpha\sigma\mu\alpha$, which signifies "modulable substance". In 1927 the physicist I. Langmuir used this term firstly to describe ionized gases. A plasma gas is, at first glance, a gas of charged particles (ions, electrons). 99% of the universe is constituted of plasmas, as for example the stars, the solar wind, the intergalactic gas, the ionosphere, the lightnings, the aurora borealis, the tails of comets, *etc*. One may say that the earth is completely surrounded by a plasma gas, which is trapped within its magnetic field. In contrast to this, in our close environment plasmas are rather rare (1%) and occur (very often under artificial form) for example in plasma screens, fluorescent lamps, electric discharges, particle accelerators, nuclear fusion, *etc*. The rest of our nearby environment occurs under solid, liquid or gaseous form. But, even if the plasmas are fairly rare in our close environment, we are, without knowing it, in permanent contact with them. Indeed, all the electromagnetic fields around us come from some object constituted of plasmas, as for example the stars or the fluorescent lamps, and even for communication on earth and with the space (satellites), plasmas (and their interaction with the magnetic fields) are of crucial importance. Thus the study of this fourth state of matter, which is the site of quiet a large variety of physical phenomena, is interesting not only for its own, but also for lots of important applications, like semiconductor technologies, plasma lasers, controlled nuclear fusion, ion propulsion rockets, gas discharges, *etc*.

The fact that the plasma is constituted of charged particles changes completely its physical behaviour as compared to the dynamics of neutral gases.
Firstly, in a neutral gas binary collisions between the particles determine entirely the global behaviour of the gas, leading to a thermodynamical equilibrium via diffusion and convective transport. These collisions are of short range, called also "hard sphere collisions". In contrast to this, in a completely ionized plasma, the collisions are of electromagnetic type, hence of long range (Coulombian force decreases as $1/r^2$). These are

FIGURE 1: Natural plasmas : sun, lightening, aurora borealis

collectives interactions, fundamentally different from hard sphere collisions. One particle is interacting with its close neighbour but also with all other particles by means of the (mean) electromagnetic fields, created by them. If the plasma is partially ionized, then also short range collisions may occur between the charged particles and the neutrals.
Other physical phenomena, such as the electromagnetic screening, instabilities, turbulence, waves, chaos *etc* contribute to the fact that the plasma constitutes a remarkable domain of study. Indeed, a sufficiently high energy is needed in order to create a plasma (from neutral atoms) or to maintain it. This energy can be furnished by heating, radiation (absorption of energetic photons) or ionization by impact with energetic electrons. Without this energy, the plasma will recombine and become a neutral gas. Hence, being so energetic, plasmas are far from a thermodynamical equilibrium and are the site of high instabilities and turbulence. This turbulence concerns, apart from the density and velocity fluctuations, also the electromagnetic fluctuations.
Moreover, while in neutral gases only one type of wave occurs, the acoustic wave, in plasmas several types of waves develop, thanks to the collective behaviour of the plasma. These waves can be divided into two categories : the transverse electromagnetic waves, as for example the Alfén waves, and the longitudinal electrostatic waves, as the Langmuir or ion acoustic waves. All these phenomena lead to very intricate plasma dynamics and it is not surprising that much of the research is devoted to the description and understanding of wave propagation in plasmas.
Finally, another complexity of plasmas consists in the fact that they are highly anisotropic, the particle dynamics as well as the propagation of the fluctuations are very different if considered in the parallel respectively perpendicular direction to the magnetic field lines.

To briefly summarize this discussion, plasmas are much more than a gas constituted of charged particles. Collective effects play an important role and the underlying physics is very different from that of neutral gases. The behaviour of a plasma is very complex, the main reason being the nonlinear and self-consistent nature of the coupled system charged-particles $\leftrightarrow$ fields.

Let us now come to the particular field of magnetically confined fusion plasmas, which are studied today in order to try to find solutions for longer-term, clean energy production. The concept of nuclear transformations, like fusion and also fission, is to

create high binding energy nuclei, from lower ones, such that the energy difference is released. The thermonuclear fusion is a process which joints together two (or several) light atomic nuclei to build a heavier nucleus, the rearrangement resulting in a reduction of the total mass, which is transformed in energy via $E = mc^2$. In contrast to this, the nuclear fission is a process which splits a heavy nucleus in lighter ones, releasing again energy according to the mass-energy equivalence. Fission reactors are the common type of today's nuclear reactors. Fusion reactors, which try to mimic the physical phenomenon occurring in the centre of the sun and other stars, are in intensive study today, with the hope to develop a reliable, illimitable, clean power production system. The ambition is to construct a reactor which does not produce greenhouse gases, whose waste products are non-radioactive (ideally) and which comprises/possesses no explosion risk (no runaway reactions).

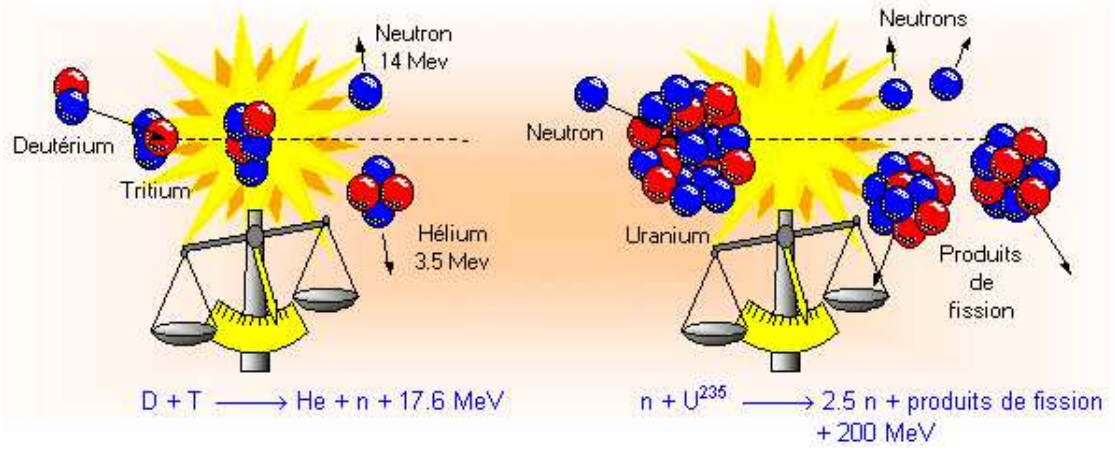

FIGURE 2: Fusion (left) and fission (right) reactions
(http ://www-fusion-magnetique.cea.fr)

The following Deuterium ($D = H^2$)-Tritium ($T = H^3$) reaction

$$D + T \rightarrow He^4 + n + 17,6\, MeV\,,$$

is retained at the moment for the fusion reaction, as it has the highest probability of fusion if compared to other fusion reactions, and as it reacts at lower temperatures also. As a result of this reaction, an α-particle is produced and a neutron released. The energy of the α-particle is used to sustain the necessary reaction temperature of the plasma, while the energy of the neutron is captured to produce energy.

The main difficulties in this fusion process are the following :

— the energy has to be high enough, in order to overcome the Coulomb repulsive force between the atomic particles, such that the attractive nuclear force can bind them into the new nucleus ($\sim$ hundred million kelvin, $\sim 15\, keV$)

— the confinement has to be strong enough, in order to avoid the dispersion of the energetic plasma and thus to permit the fusion process to occur

— more energy has to be produced than it is furnished to the system and moreover the process has to be self-sustained.

In summary, the essential physical challenges with fusion consist in finding the manner to sustain through time a far from equilibrium, unstable plasma gas. Confinement is determined by the balance between the magnetic and pressure forces, however the occurrence of instabilities can generate a plasma transport across the magnetic field lines, leading to a loss of energy as well as high surface temperatures. Thus, one has firstly to understand and control the high turbulent transport processes, in order to avoid the deconfinement of the plasma gas, and secondly to control the plasma edge (understand the complex plasma-wall interactions), in order to prevent the introduction of impurities in the core of the plasma and besides to avoid the deterioration of the wall materials. The most promising fusion reactor in study at present is the ITER tokamak (International Tokamak Experimental Reactor) in Cadarache, France.

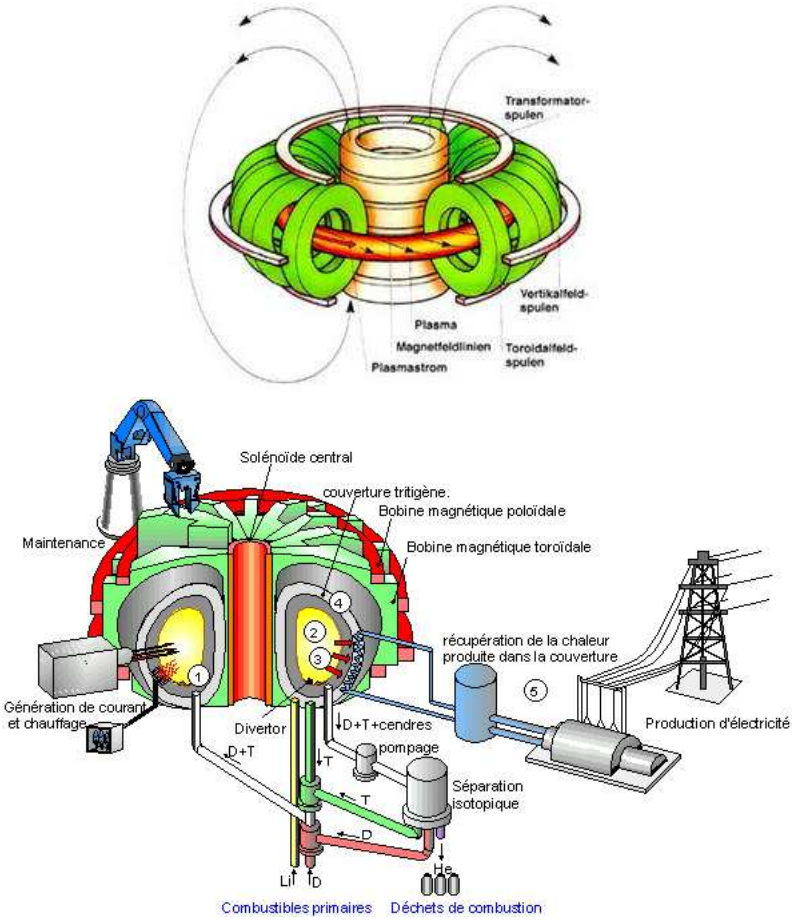

FIGURE 3: Fusion reactors, tokamaks. (http ://www-fusion-magnetique.cea.fr/)

The just described thermonuclear fusion process occurs naturally in stars, in particular in our own Sun. The Sun is a "dwarf" star of average size, temperature and brightness, held together by its own gravity, in other words it is a self-gravitating sphere

of plasma. The interior of the Sun is divided into three regions, defined by the different processes that occur there (see Fig. 4). First, there is the core, where the nuclear fusion reactions take place, turning hydrogen nuclei into helium nuclei. These reactions release the energy that escapes from the sun surface as visible light. On its way towards the Sun's surface, this energy is firstly transported by radiation (photons) through the radiative zone, a phenomenon which takes about a million years, due to the high density of the Sun's interior. As the temperature gets lower, the radiation becomes less significant and another process is set into motion in order to transport the energy, the convection. It is thought that most of the magnetic activity of the sun is driven by turbulent flows, rotation and shear in this convective zone and the origin of the magnetic field is believed to be in the tachocline, which is the thin interface layer between the radiative zone and the convective one. Anyhow, the dynamics of the Sun's interior is up to now still poorly understood. Given the wide range of temporal and spacial scales coexisting in the physical processes in the Sun, it is a great challenge to model self-consistently the solar interior and the dynamo effects. All these phenomena require state-of-the art numerical schemes supported by rigorous mathematical results.

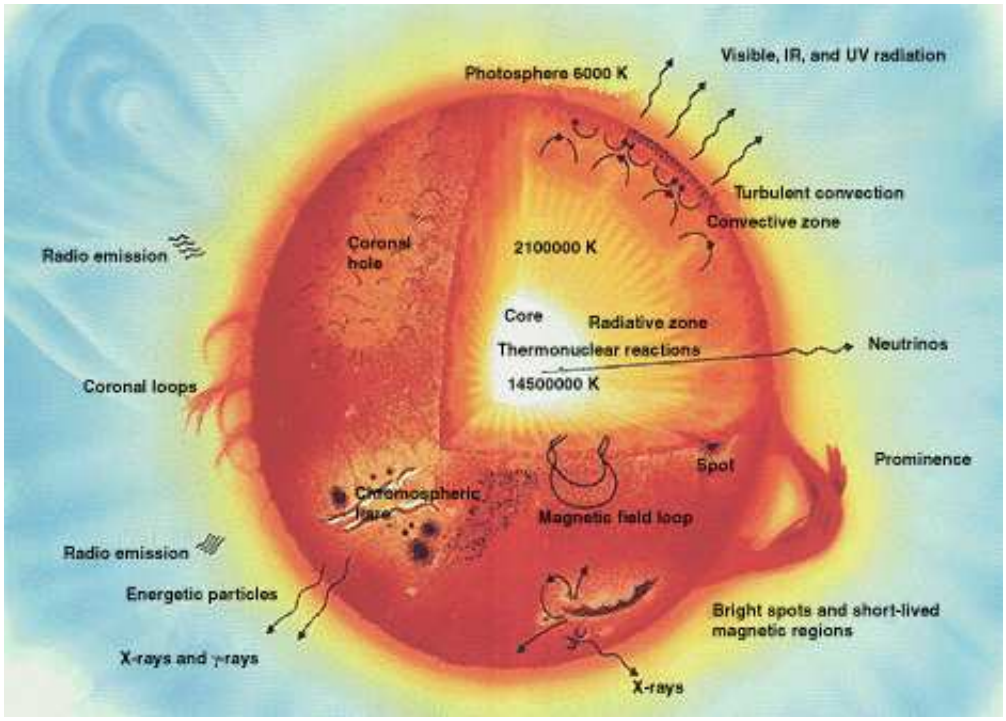

FIGURE 4: Schematic representation of the Sun's interior (http ://www.futuretimeline.net)

0.1 Different mathematical descriptions

Different approaches can be used in order to describe the dynamics of a large number of particles interacting with each other, in particular to describe the evolution of charged

particles in a self-consistent electromagnetic field. For example, one can distinguish between :

— the particle description, based on the laws of motion of classical mechanics (Newton's laws) for the description of each individual particle movement ;
— the kinetic description, based on a collective plasma description via the particle distribution function $f_{e,i}(t,x,v)$;
— the fluid description, describing the plasma in terms of averaged macroscopic quantities, depending only on t and x.

These successive models differ in complexity and precision. They are increasingly simplified, in the sense that they can be obtained from one another by decreasing the number of degrees of freedom, hereby becoming less accurate. Depending on the physical phenomenon one wants to investigate, one has to choose within all these models the one which is the most accurate with respect to the particular physical situation, paying attention at the same time to the numerical costs.

The first model, the particle dynamic model, is the most intuitive one and the physically most accurate one, but also the most inadequate/heavy from a numerical point of view. The evolution of each particle is described by means of Newton's law, $F = m\,a$, coupled to Maxwell's equations for the electromagnetic fields (E,B). To be more precise, let us consider N particles interacting with each other, located at instant t at the positions $x_i(t)$ and evolving with speeds $v_i(t)$ for $i = 1,...,N$. Newton's laws, describing their evolution, write now as a system of coupled ODEs, namely

$$\begin{cases} x_i'(t) = v_i(t) \\ m_i v_i'(t) = F_i(t, x_1, ..., x_N, v_1, ..., v_N)\,, \end{cases} \qquad \forall i = 1,...,N\,, \tag{1}$$

with m_i the mass of particle i and F_i the force exerted on this particle i by the other particles or an external field.

— As an example, we can consider the forces as obtained from a potential :

$$F_i = -\nabla_{x_i}\Phi(t, x_1, ..., x_N)\,,$$

with Φ describing both binary interactions between particles and the influence of an external environment :

$$\Phi(t, x_1, ..., x_N) = \frac{1}{2}\sum_j \sum_{k\neq j} \Phi_{int}(x_j - x_k) + \sum_j \Phi_{ext}(t, x_j).$$

Thus,

$$F_i(t, x_1, ..., x_N) = \sum_{k\neq i} F_{int}(x_i - x_k) + F_{ext}(t, x_i)\,,$$

$$\text{with} \quad F_{int} = -\nabla\Phi_{int} \quad \text{and} \quad F_{ext} = -\nabla\Phi_{ext}\,.$$

A standard example of an interspecies force is $F_{int}(x) := C\frac{1}{|x|^s}\frac{x}{|x|}$, where $s = 7$ represents the Van der Waals forces between molecules, and with $s = 2$ one has the electrical Coulomb force.

— We can also consider forces such as the Lorentz force in plasma physics, induced by external and self-induced electromagnetic fields :

$$F_i(t, x_i, ..., x_N, v_1, ..., v_N) = \mathfrak{q} \sum_{k \neq i}^{N} (E_k(t, x_i) + v_i \times B_k(t, x_i)) \ ,$$

where $E_k(t, x_i)$ resp. $B_k(t, x_i)$ represent the electric resp. magnetic fields generated at the position x_i by the particle located at the position x_k and $\mathfrak{q}$ stands for the electron resp. ion charge.

A complete dynamical description of the whole particle-system via these Newton's laws is however out of reach, as the system contains $6N$ degrees of freedom, where N is the number of particles, which is of the order of Avogadro's number, *i.e.* 10^{23}. No computer today can deal with such high dimensionalities, such that this approach remains purely theoretical. Taking such large numbers into account requires definitively new models and concepts.

The point is that usually one is not interested in the whole microscopic information incorporated in all the particle trajectories, but much more in the collective behaviour of the system. A mesoscopic picture emerges, aimed to simplify the previous particle model in order to get a reduced pricture, preserving however all the interesting physics. The main idea is to average out some unnecessary information and consider a statistical picture of the gas of electrons/ions. The plasma dynamics is described via a distribution function $f(t, x, v)$, with $f(t, x, v)\, dv\, dx$ representing the number of particles to be found at time t in the infinitesimal phase-space volume $dv\, dx$ around (x, v). The equation governing this particle distribution function is a kinetic equation, of the form

$$\partial_t f + v \cdot \nabla_x f + \frac{F}{m} \cdot \nabla_v f = Q(f) \, , \tag{2}$$

called the Vlasov equation if $Q \equiv 0$ respectively the Boltzmann or Fokker-Planck equation, depending on the form of the used collision operator $Q(f)$. If $F(t, x, v) = E(t, x) + v \times B(t, x)$ is the Lorentz force in plasma physics, the kinetic equation has to be coupled self-consistently with Maxwell's equations for the computation of the electromagnetic fields (E, B) or Poisson's equation in the case the magnetic field B is given. Indeed, taking into account for two species, electrons and ions, the phase-space particle distribution function $f_\alpha(t, x, v)$ (where α stands either for the electrons $\alpha = e$ or for the ions $\alpha = i$) evolves accordingly to the Boltzmann equation

$$\partial_t f_\alpha + v \cdot \nabla_x f_\alpha + \frac{e_\alpha}{m_\alpha}(E + v \times B) \cdot \nabla_v f_\alpha = Q(f_\alpha) \, , \tag{3}$$

where $e_\alpha = \pm e$ resp. m_α are the particle elementary charge resp. mass and $E(t, x)$ resp. $B(t, x)$ are the electric respectively magnetic fields, determined self-consistently from

Maxwell's equations

$$\begin{cases} \nabla \cdot E = \dfrac{1}{\varepsilon_0}\rho \\ -\dfrac{1}{c^2}\partial_t E + \nabla \times B = \mu_0 j \\ \partial_t B + \nabla \times E = 0 \\ \nabla \cdot B = 0\,, \end{cases} \tag{4}$$

where ε_0, μ_0 and $c := (\varepsilon_0\,\mu_0)^{-1/2}$ are the free-space permittivity, permeability resp. speed of light and where the charge and current densities are computed via

$$\rho(t,x) = \sum_\alpha e_\alpha \int_{\mathbb{R}^3} f_\alpha(t,x,v)\,dv = e(n_i - n_e)\,, \quad j(t,x) := \sum_\alpha e_\alpha \int_{\mathbb{R}^3} v\, f_\alpha(t,x,v)\,dv\,.$$

In the electrostatic case ($B = 0$), Maxwell's equations (4) have to be replaced by Poisson's equation

$$-\varepsilon_0 \Delta \Phi = \rho\,, \tag{5}$$

where Φ is the electrostatic potential, related to the electric field E by $E = -\nabla\Phi$, where the sign comes from the convention that the electric field points in the direction of the ion motion.

Although the precise locations of the individual particles are lost in the kinetic theory, detailed knowledge of the particle motion is still incorporated. However, even if the kinetic models (2) are simpler than the particle models (1), they are used at the moment mainly on a theoretical level, as the numerical costs are still rather high, the system being 6 dimensional. They are generally the starting point for the derivation of more tractable macroscopic models, via asymptotic limits or moments methods.

The third approach is the macroscopic or fluid approach. The fluid models constitute a further simplification of the previous kinetic models (2), and are hence numerically more attractive, but poor from a physical point of view. They deal with averaged quantities, like the particle density $n(t,x)$, the current density $j(t,x)$, the velocity $u(t,x)$, the temperature $T(t,x)$, the total energy $W(t,x)$, which only depend on the position and the time variable. The equations describing the evolution of these quantities are the following conservation laws

$$\begin{cases} \partial_t n + \nabla_x \cdot (n\,u) = 0 \\ \partial_t (n\,u) + \nabla_x \cdot (nu \otimes u) + \dfrac{1}{m}\nabla_x \cdot \mathbb{P} = \dfrac{\mathfrak{q}}{m}\, n\,(E + u \times B)\ , \\ \partial_t W + \nabla_x \cdot (W\,u + \mathbb{P}\cdot u + q) = \mathfrak{q}\, nu \cdot E \end{cases} \tag{6}$$

with (E, B) again given by Maxwell's (or Poisson's) equations. Here $\mathbb{P}$ denotes the pressure tensor and q is the heat flux. For $E \equiv 0$ and $B \equiv 0$ one recognizes the form of the Navier-Stokes model. Even if physically not so accurate, fluid models are still of wide use at the moment in plasma simulations, as they permit more easily to make use of the physical intuition one has and are numerically less demanding. Moreover, they permit

to use the knowledge and the numerical codes from the fluid domain, adapting them however to the new "gas", as the plasma lacks the high collisionality of the fluids as well as their isotropy. However, one has to keep in mind that the extraordinary varied plasma behaviour (as for example plasma waves and oscillations) can only be fully captured in a kinetic framework.

In order to prepare the next section, let us precise here some important points, concerning the link between the kinetic models (2) and the fluid models (6). The macroscopic quantites occurring in (6) (n, u, W) can be computed via an average process of the particle distribution function f in the velocity variable, namely

$$n(t,x) := \int_{\mathbb{R}^3} f(t,x,v)\, dv\,, \quad n(t,x)\, u(t,x) := \int_{\mathbb{R}^3} v\, f(t,x,v)\, dv\,, \tag{7}$$

$$\frac{3}{2} k_B n\, T := \frac{m}{2} \int_{\mathbb{R}^3} |v-u|^2\, f(t,x,v)\, dv\,, \quad W(t,x) := \frac{m}{2} \int_{\mathbb{R}^3} |v|^2\, f(t,x,v)\, dv\,, \tag{8}$$

$$\mathbb{P}(t,x) := m \int_{\mathbb{R}^3} (v-u)\otimes(v-u)\, f(t,x,v)\, dv\,, \quad q(t,x) = \frac{m}{2} \int_{\mathbb{R}^3} (v-u)\, |v-u|^2\, f(t,x,v)\, dv\,. \tag{9}$$

The pressure tensor is usually decomposed into the scalar, hydrostatic pressure part and the viscous stress tensor, *i.e.* $\mathbb{P} = p\, Id - \mathbb{S}$. The stress tensor $\mathbb{S}$ is a measure of the extent to which the gas deviates from an isotropic state.
The just introduced macroscopic quantities (7)-(9) constitute the bridge between the kinetic theory and the fluid one, however if one looks in more details, you can remark that the fluid model (6) is not complete. In order to have a closed fluid model (6) one has to find relations linking the higher order moments of f, namely $\mathbb{P}$ and q, to the quantities (n, u, T) or equivalently (n, u, W). This is the so-called "closure problem" in the fluid approach, and it is far from being a harmless problem, as it is not always possible to find such relations. The Navier-Stokes model is based on the following "empirical" closure relations :

$$\begin{aligned}
&q = -\kappa\, \nabla_x T \qquad \text{(Fourier's law)}\\
&\mathbb{S} = \mu \left[\nabla_x u + (\nabla_x u)^t - \frac{2}{3} (\nabla_x \cdot u)\, Id \right] + \eta (\nabla_x \cdot u)\, Id \qquad \text{(Newton's law)}\\
&p = n\, k_B\, T \quad \text{(perfect gas)}\,; \quad p = c\, n^\gamma\,,\ \gamma := c_p/c_V \qquad \text{(isentropic equation of state)}\,,
\end{aligned} \tag{10}$$

which are established via first principle physical considerations, deep insight in the phenomenon, guesswork, experience and experiments. These empirical approaches have however limited success for complexe systems, like turbulent flows. Doubtlessly it would be more appropriate to obtain such closures via rigorous or at least formal asymptotic arguments, starting from the kinetic description (2). But mathematical rigorous derivations of such constitutive relations are relatively rare and usually carried on only for specific simplified problems. The closure problem underlines somehow the fact that the fluid/macroscopic quantities contain less information than the kinetic distribution function. To summarize this section, the hierarchy of the different mathematical models presented above as well as the relations within them, are sketched in Figure 5.

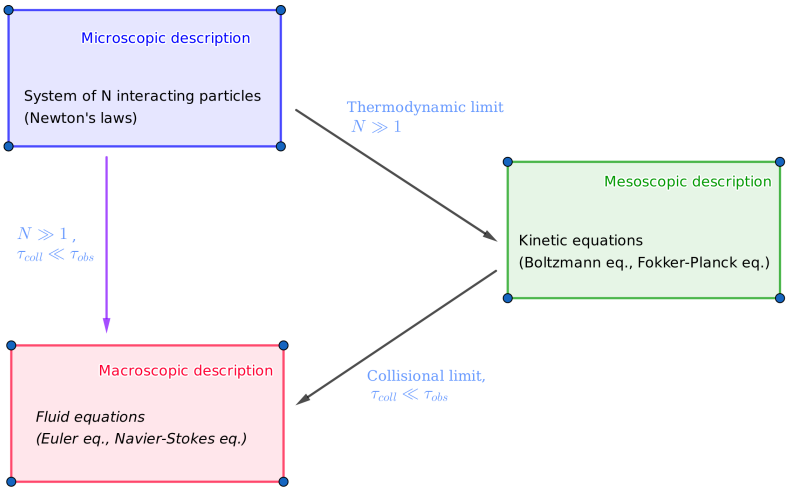

FIGURE 5: Hierarchy of the different mathematical descriptions.

0.2 Multiscale problems

We are intended now to give some precisions about multiscale problems, in particular about the mathematical and numerical methods for the study of such problems. We have seen in the previous section that a phenomenon can be described on different levels of accuracy. The main interest is to solve (as precise as possible) real-life problems, with their specificities. For this, it is important to find out which type of particularity has a problem, and which type of theoretical resp. numerical approach is to be chosen, in order to remain close to reality and also pragmatic.

Plasma dynamics is characterized by a multiscale nature. Magnetism creates anisotropy, which means that the properties of the plasma are rather different when considered in the parallel or in the transverse direction with respect to the magnetic field lines. This anisotropy contributes, jointly with other phenomena, to the multi-scale dynamics of the plasma, in particular a very large variety of time and space scales occurs (see Fig. 6). As an example, concerning the temporary scales, one can pass from the fast electron plasma frequency ω_p, to the fast Larmor gyromotion ω_c, further to the collisional frequencies $\nu_{i,e}$ and finally to the confinement time τ_E . Concerning the spatial scales, it ranges from the small Debye length λ_D, to the electron Larmor radius ρ_e, further to the mean free path of the particles and finally to the spacial extent of the tokamak L.

Many other problems in nature exhibit multiscale behaviours, which can be rather different in character. One can divide these problems in two categories. On one hand we have problems which exhibit local singularities, like for example boundary or internal layers, shocks, dislocations and so on. On the other hand we have problems, where micro-

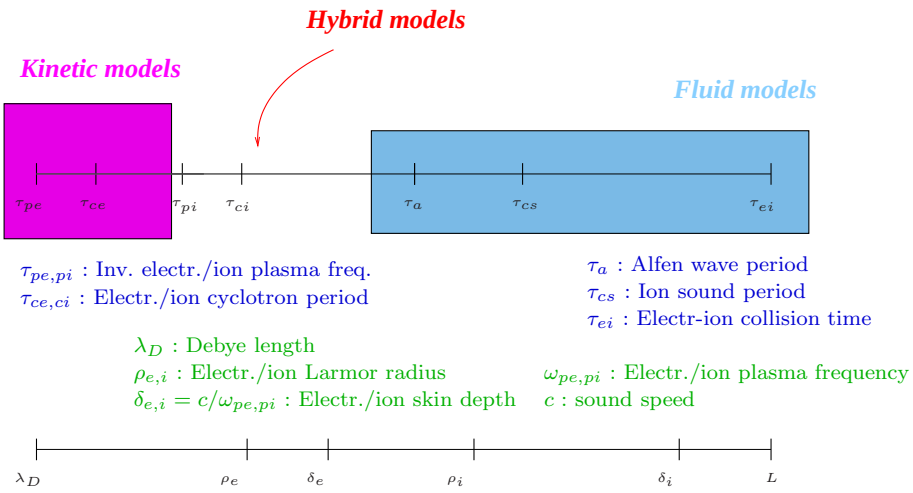

FIGURE 6: Different time and space scales occurring in a fusion plasma

scopic and macroscopic scales coexist in the whole domain, as for example porous media flows, turbulent flows, highly oscillating problems *etc.* A general, unified treatment of all these problems is impossible, such that a lot of techniques have been developed in literature, each one being adapted to a particular situation.

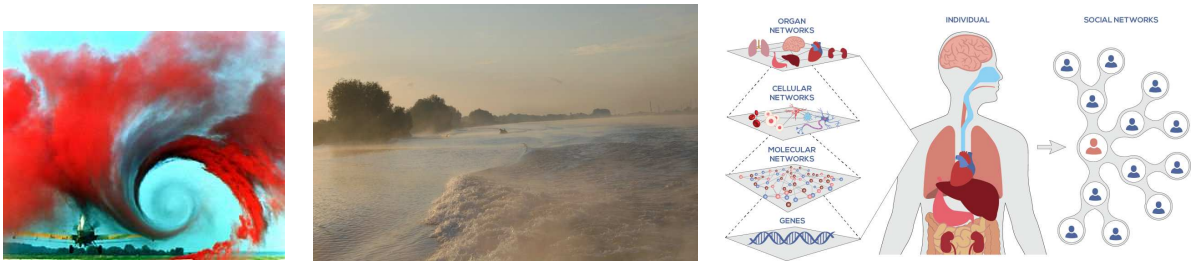

FIGURE 7: Multi-scale phenomena in nature

The theoretical and numerical treatment of problems with multiple scales has always been far from being trivial. The study requires a lot of theoretical/numerical skills, physical insight into the problem to be studied and also intuition and experience. When several scales occur in a problem, it is no more adequate to use the so-called "traditional approaches" which describe the phenomenon on a single scale. Indeed, describing the problem on a microscopic level (for ex. particle or kinetic level) is physically very accurate, however from a computational point of view unfeasible. Using on the other hand a macroscopic description (fluid models), which describes the macroscopic system evolution, eliminating the microscopic informtaion, is also inappropriate. In point of fact, this procedure uses often empirical closures for the elimination/description of the microscopic scales, that are not justified nor well understood, as for example the viscosity tensor terms in turbulent flows (see (10)). In all these cases, it could be more appropriate to employ a multiscale technique, for example by making use of different models, which describe the various phenomena on their different scales, and coumpling

them somehow ; and all this by taking care to achieve a balance between accuracy of the numerical results and efficiency of the numerical method. Briefly, the main goal of multiscale techniques is to design microscopic-macroscopic numerical methods, which are more efficient than solving the full microscopic model and at the same time furnish the desired accuracy.

To be more precise, suppose we are interested in the evolution of a macroscopic quantity, say U (representing for ex. (n, u, T) in (6)), but we do not have an explicit macroscopic model for the description of U, which is valid everywhere. This can be either because we lack the constitutive relations (as (10)) or because the macroscopic model is invalid due to the presence of localized singularities for example. However, we dispose of a microscopic model, describing the dynamics of a microscopic quantity u (for ex. f in (2)), which is related to U by a relation $F(u) = U$ (see (7)-(9)). Our ultimate goal is to accurately approximate the variable U, using a macroscopic grid, in order to be efficient from a computational point of view. A standard method would require to use a fine grid, in order to resolve the small scales of the problem, obtaining thus u, and computing then the correct macroscopic solution via the function $F(\cdot)$. However, this is usually a computationally phenomenal and unfeasible work. And moreover, for most engineering purposes, it is even unnecessary to know all the details of u. Engineers are often contented with accurate time-averaged properties of the flow, as the averaged velocities, pressures *etc.*

Multi-scale methods were thus introduced in literature, based on different ideas, however with the same aim, which is to capture the macroscopic evolution, using the indispensable microscopic information, without however having to resolve in detail this microscopic behaviour. Some analytical techniques to cope with multiscale problems are for example the *matched asymptotics method*, used for problems which undergo rapid variations in localized regions, or the *homogenization methods*, employed in the case of problems with oscillating coefficients and based on asymptotic expansions. Among the numerical approaches can be counted the *multigrid methods* and the *adaptive mesh refinements*, which are efficient techniques for the resolution of the small-scale behaviour of the solution. Furthermore, *domain decomposition methods* aim to couple different mathematical descriptions, corresponding to different regions of the domain, where the physics is distinct. And finally, *multiscale finite element methods* employ basis functions, which incorporate the small-scale information, permitting thus the use of coarse grids. For a detailed description of all these methods, we refer to the textbooks [30, 38, 45] as well as all the references therein.

Briefly, multiscale techniques consider simultaneously models at different levels, hoping to develop an approach that shares the efficiency of the macroscopic models as well as the accuracy of the microscopic models. As we saw, asymptotic analysis and numerical techniques are the two principle techniques to investigate multiple scale problems. The question is if there may be other ways to attack multiple scale problems, ways for example that combine both techniques and could be more efficient. We shall present in the next section such a new technique, the AP-strategy, which performs a fundamental change in the way one understands multiscale modelling.

0.3 Asymptotic-Preserving techniques

Among multi-scale problems one encounters very often singularly perturbed problems, which clearly reveal a multiscale character, and the numerical resolution of whom presents some major difficulties. Singular perturbation problems are characterized by the occurrence of one or several small parameters, denoted in this section by $0 < \varepsilon \ll 1$, and the mathematical as well as numerical difficulties arise due to a change in type of the equation as $\varepsilon \to 0$. The solutions of the singularly perturbed problem show a non-uniform behaviour as the parameter tends to zero, for instance the character of the limiting solution is different in nature from that of the solutions for finite values of $\varepsilon > 0$. Examples of such singularly perturbed problems are viscous flows with large Reynolds numbers, convective heat transport with large Peclet numbers, low Mach number flows, diffusive relaxation in kinetic models and so on.

The Asymptotic-Preserving schemes are efficient procedures for solving singularly perturbed problems P^ε. The solution of P^ε is supposed to converge, as the perturbation parameter tends to zero, towards the solution of a limit problem P^0, which is a well-posed problem. However, the fact that the singular limit $P^\varepsilon \to_{\varepsilon\to 0} P^0$ leads to a change in the type of the equation, explains somehow the difficulties encountered when trying to solve P^ε for too small ε-values. The use of standard numerical schemes for the resolution of singularly perturbed problems requires very restrictive time and space dicretization step conditions, of the type $\Delta t, \Delta x \sim \mathcal{O}(\varepsilon)$ or $\Delta t, \Delta x \sim \mathcal{O}(\varepsilon^2)$, due to stability reasons. This becomes rapidly too costly from a numerical point of view and consequently a numerical asymptotic study and even numerical simulations for small ε-values, are out of reach. Moreover, standard implicit schemes (even if computationally heavy) may be uniformly stable for $0 < \varepsilon < 1$, but yet provide a wrong solution in the limit $\varepsilon \to 0$, which means the scheme is not consistent with the limit problem P^0. Thus the design of robust numerical methods for singularly perturbed problems, whose accuracy does not depend on the parameter ε (hence on the local scales of the singularity), allowing even to capture the limit $\varepsilon \to 0$, becomes an important task.

In order to tackle such problems, several methods were introduced in literature. One approach can be to solve directly the limit problem P^0 instead of P^ε, if ε is small. However, in some situations, the parameter ε can vary within the simulation domain, making thus this approach unusable. Indeed, ε is the ratio of two characteristic lengths, which can vary in space as well as in time. In this case, hybrid techniques can be employed, solving P^ε there where $\varepsilon \sim \mathcal{O}(1)$ and P^0 where ε is rather small. Several difficulties can be encountered with this approach, for example how to locate the interface between P^ε and P^0 and what type of interface conditions to use. Thus, this approach can be difficult to implement in practice.

Asymptotic-Preserving schemes were introduced the first time by S. Jin [40] with the aim to cope with such singularly perturbed problems, in particular in the framework of kinetic models in a diffusive regime. The construction of these AP-schemes necessitates the existence of a well-posed limit problem P^0, which has to be identified beforehand. The main feature of these schemes is that they permit a precise, ε-independent, resolu-

tion of the problem P^ε as well as of its limit problem P^0, with no huge computational effort. The main idea for the construction of AP-schemes is based on asymptotic arguments and consists in a mathematical reformulation of the singularly perturbed problem P^ε into an equivalent problem $(AP)^\varepsilon$, which is a regular perturbation of the limit problem P^0. The equivalent reformulation of P^ε into $(AP)^\varepsilon$ is a sort of "reorganization" of the problem into a form which is better suited for the numerical discretization, in particular which is a regular perturbation of P^0. The same numerical scheme is then used for the discretization of P^ε as well as for P^0, which means that they allow for an automatic numerical transition from P^ε to P^0. Remark that the AP-reformulation is by no means unique, and several AP-schemes can be conceived/designed for the same problem. It is necessary to underline here that the asymptotic preserving techniques are not used to derive a simplified "macroscopic" model, which is then solved numerically. Rather the objective is to construct a numerical scheme, using asymptotic techniques, whose solution does not deteriorate as the singular limit is approached.

To summarise, the essential properties of AP-schemes are (see diagram 8) :
— for fixed $\varepsilon > 0$, the AP-scheme, denoted in this diagram $P^{\varepsilon,h}$, is a consistent discretization of the continuous problem P^ε, where $h = (\Delta t, \Delta x)$
— the stability condition is independent of ε
— for fixed discretization parameters $h = (\Delta t, \Delta x)$, the AP-scheme $P^{\varepsilon,h}$ provides in the limit $\varepsilon \to 0$ a consistent discretization of the limit problem P^0

Thus, the asymptotic-preserving approach consists somehow in trying to mimic on the discrete level the asymptotic behaviour of the singularly perturbed problem solutions. It is thus very important to have a full understanding of the solutions behaviour. Remark that the AP-techniques have to be distinguished from the multiscale techniques, as the former solve the micro-scales when the (spacial or/and temporal) mesh-sizes resolve these scales and automatically switch to the macroscopic behaviour when the mesh-sizes do not resolve the micro-scales. In other words, the AP-schemes catch the numerical transition from microscopic to macroscopic scales, in some difficult situations as singularly perturbed problems, however their primary focus is not to reduce the computational costs, as the multiscale methods do.

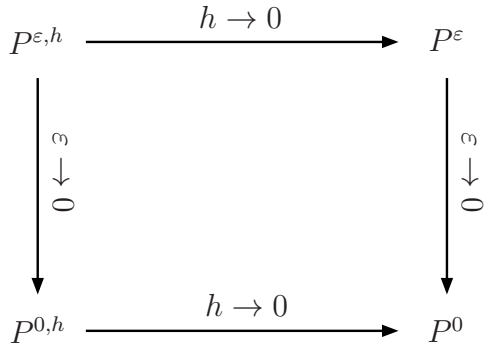

FIGURE 8: Properties of AP-schemes

0.4 Outline

The present work is a review of several Asymptotic-Preserving schemes, constructed in the kinetic and fluid framework. Inevitably, the choice of the model problems is related with the author's knowledge and with the concept of providing the reader with the most important features of AP-schemes. These schemes can be designed for several other singularly perturbed problems, that admit asymptotic behaviours/regimes.

An overview of the subject of this manuscript is :

— Chapter 1 introduces the kinetic equations and the transition towards the fluid models ;
— Chapter 2 deals with the Boltzmann equation in the drift-diffusion limit ;
— Chapter 3 discusses the Boltzmann equation in the hydrodynamic limit ;
— Chapter 4 treats the subject of the Boltzmann equation in the high-field limit ;

Chapitre 1

Kinetic models and transition towards the fluid approach

The main objective of the kinetic theory is the modelling of a large number of identical particles (rarefied gas for example) interacting with each other via different types of forces to be specified. The cloud of particles is described via a (probability) density function $f(t,x,v)$, where $f(t,x,v)\,dxdv$ represents the number of particles arising at instant t in the phase-space volume $dxdv$ around the point (x,v). Underlying kinetic theory is the modelling assumption that the gas is constituted of sufficiently many particles, such that it can be treated as a continuum. However, too many particles collinding with each other would instead lead to a more macroscopic, fluid description. There are two ways to consider f : it can be seen as the density of the gas in the phase-space (x,v) or rather as a probability density, which reflects somehow our lack of knowledge of the true positions and velocities of the particles. Both points of view are often found in literature and have no consequence on the following theory.
In the following we shall explain how the Vlasov and the Boltzmann equation, *i.e.*

$$\partial_t f + v\cdot\nabla_x f + \frac{F_{ext}+F_{mf}}{m}\cdot\nabla_v f = Q(f,f)\,, \tag{1.1}$$

is obtained from the underlying microscopic model, namely Newton's laws for the description of the trajectory of each particle. As (1.1) suggests, the evolution of the density function f is determined by the flow in the phase-space under the influence of an external and a self-consistent force field $F = F_{ext} + F_{mf}$ and by the effect of collisions, described by the collision operator $Q(f)$.

1.1 Kinetic models for non-interacting particles

Let us start by trying to get the Vlasov equation from the fundamental Newton's laws, and this in the simple case of non-interacting particles, evolving in a given exterior force field F_{ext}, which satisfies the divergence-free condition, *i.e.*

$$\nabla_v\cdot F_{ext} = 0\,.$$

The particles issued from the phase-space point (ξ, η) follow the trajectory, given by the ODE (Newton's laws)

$$\begin{cases} X'(t) = V(t) \\ m\, V'(t) = F_{ext}(t, X(t), V(t))\,, \end{cases} \qquad \forall t \in \mathbb{R}\,, \tag{1.2}$$

with initial condition $(X(0), V(0)) = (\xi, \eta) \in \mathbb{R}^d \times \mathbb{R}^d$, where $d = 3$ is the dimension of the (position and also velocity) space. The solution of this ODE will be denoted by $(X(t; 0, \xi, \eta), V(t; 0, \xi, \eta))$, enforcing the dependence on the initial condition. Let us denote the flow corresponding to (1.2) by Φ_t, *i.e.*

$$\Phi_t : (\xi, \eta) \in \mathbb{R}^{2d} \to (X(t; 0, \xi, \eta)), V(t; 0, \xi, \eta))) \in \mathbb{R}^{2d}\,,$$

and by J_t its Jacobian, namely $(J_t)_{kl} = \partial_k (\Phi_t)_l$. Remark that $t \in \mathbb{R}$ is here an arbitrary but fixed parameter, and for simplicity reasons, let us denote in the rest of this subsection simply by (x, v) the end-point of the mapping $\Phi_t(\xi, \eta)$, at this fixed time instant. The flow Φ_t is volume-preserving in the phase space, due to the divergence-free property of the force-field. Indeed, one can show that $\det(J_t) \equiv 1$. Denoting now for an initial domain $\omega \subset \mathbb{R}^{2\,d}$ the volume following the field lines by $\Omega_t := \Phi_t(\omega)$, one has

$$|\Omega_t| = \int_{\Omega_t} 1 dx\, dv = \int_{\omega} \det(J_t(\xi, \eta))\, d\xi\, d\eta = |\omega|\,,$$

where $|\cdot|$ stands for the measure of a domain. The same variable-change leads, at a fixed but arbitrary time instant $t \in \mathbb{R}$, to

$$\int_{\Omega_t} f(t, x, v)\, dxdv = \int_{\omega} f(t, \Phi_t(\xi, \eta))\, d\xi\, d\eta\,.$$

But the number of particles "encapsulated" in the volume Ω_t is constant in time, as we suppose that there is no creation and no destruction of the particles during the evolution, but only transport along the field lines associated to the ODE (1.2). Thus one has

$$\frac{d}{dt}\left[\int_{\Omega_t} f(t, x, v)\, dxdv\right] = 0\,,$$

which leads to

$$\begin{aligned} &\frac{d}{dt}\left[\int_{\omega} f(t, \Phi_t(\xi, \eta))\, d\xi\, d\eta\right] = \int_{\omega} \left[\partial_t f(t, \Phi_t(\xi, \eta)) + \nabla_{x,v} f(t, \Phi_t(\xi, \eta)) \cdot \frac{d}{dt}\Phi_t(\xi, \eta)\right] d\xi d\eta \\ &= \int_{\omega} \left[\partial_t f(t, \Phi_t(\xi, \eta)) + v \cdot \nabla_x f(t, \Phi_t(\xi, \eta)) + \frac{F_{ext}(t, x, v)}{m} \cdot \nabla_v f(t, \Phi_t(\xi, \eta))\right] d\xi d\eta = 0\,. \end{aligned}$$

Now, remembering that $(x, v) = \Phi_t(\xi, \eta)$ and due to the fact that $\omega \subset \mathbb{R}^{2d}$ was arbitrarily chosen, the last equation leads finally to

$$\partial_t f + v \cdot \nabla_x f + \frac{F_{ext}}{m} \cdot \nabla_v f = 0\,.$$

1.2 Kinetic models for interacting particles

We shall now pass to the second step, taking into account interactions between the particles. We have to distinguish between short range and long range interactions, which are modeled in a different way.

1.2.1 Short range interactions or collisions

A **collision** describes the interaction process between particles, which become so close that their trajectories are greatly deflected in a very short amount of time, in the manner of billiard balls (hard sphere model). These type of interactions are modeled via a collision operator $Q(f)$, for ex. the Boltzmann collision operator we shall introduce now.

For this let us first make several postulates.

— **Binary collisions :** We shall assume that the gas is sufficiently dilute, such that a collision involves only two particles (in other words many-particle collisions will be neglected) ;

— **Localized collisions :** We assume furthermore that the collisions are localized both in space and time (the collision happens instantaneously) and (t, x) shall be considered only as a parameter, the collision having only an influence on the particle velocities ;

— **Elastic collisions :** Momentum and energy are supposed to be preserved during a collisional process. This will permit to compute the post-collisional velocities (v', v'_*) from the pre-collisional ones (v, v_*). Indeed, the conservations can be written as

$$\begin{cases} v + v_* = v' + v'_* \,, \\ |v|^2 + |v_*|^2 = |v'|^2 + |v'_*|^2 \,. \end{cases}$$

These are $d + 1$ scalar equations ($d = 3$ being the dimension of the velocity space) for $2\,d$ unknowns, such that the solution will be expressed in terms of $d - 1$ parameters. One convenient representation of this solution is given via the parameter $\sigma \in \mathbb{S}^{d-1}$ as follows

$$\begin{cases} v' = \dfrac{v + v_*}{2} + \dfrac{|v - v_*|}{2}\,\sigma \,, \\ v'_* = \dfrac{v + v_*}{2} - \dfrac{|v - v_*|}{2}\,\sigma \,, \end{cases} \tag{1.3}$$

where $\mathbb{S}^{d-1} := \{u \in \mathbb{R}^d \ / \ |u| = 1\}$ is the unit sphere. Figure 1.1 represents one collision in the velocity space, and we remark that σ represents somehow the collisional direction.

— **Micro-reversibility :** The micro-reversibility of the collisions is related to the time-reversibility of the microscopic particle dynamics. That means, we assume that during a collisional process the probability that the velocities (v, v_*) are changed into (v', v'_*) is the same as the probability that (v', v'_*) are changed into (v, v_*).

— **Molecular chaos :** We shall finally suppose that before the collision the two colliding particles are uncorrelated. It is exactly this properties which induces a time-arrow into the system, or in other words which creates an asymmetry between the past and the future, as after the collision, the particles become correlated due to the relation (1.3). due to this hypothesis the kinetic equation will no more be time-reversible.

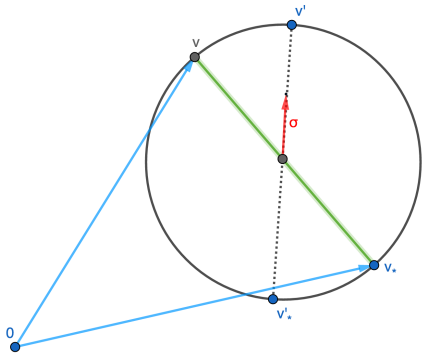

FIGURE 1.1: Sketch of a collision.

Under these five postulates we shall now derive the Boltzmann collision operator. Each one of these five assumptions will be visible in this operator. The Boltzmann collision operator describes the rate of change of the particle distribution function $f(t,x,v)$ during a small time-interval dt, due to collisions. It has the form

$$Q(f,f)(t,x,v) := \int_{\mathbb{R}^3}\int_{\mathbb{S}^{d-1}} b(v-v_*,\sigma)\,(f'\,f'_* - f\,f')\,d\sigma\,dv_*\,, \tag{1.4}$$

where we used the standard notation $f' := f(t,x,v')$, $f'_* := f(t,x,v'_*)$ and $f_* := f(t,x,v_*)$ and the formula (1.3) relating (v',v'_*) to (v,v_*,σ). The function $b(v-v_*,\sigma)$ is the so-called **collisional kernel** and describes the probability that two colliding particles, arriving with respective velocities v and v_*, will collide with "direction" σ. This collisional kernel b is determined by the microscopic (molecular) physics and is related to the so-called **cross section** Σ by the relation $b(v-v_*,\sigma) = |v-v_*|\,\Sigma(v-v_*,\sigma)$. To understand better the effect of the collision operator, one remarks that it can be split into a "gain" and a "loss" term, namely

$$Q(f,f)(t,x,v) = Q^+(f,f) - Q^-(f,f)\,,$$

where $Q^-(f,f)(t,x,v)\,dv\,dt$ gives the number of particles which are lost during the time-interval dt from the volume dv centered in v, due to a collision with another particle of velocity v_*. On the other hand $Q^+(f,f)(t,x,v)\,dv\,dt$ counts the particles which enter the volume dv centered in v during a collisional process involving two particles with velocities (v',v'_*). Here the product $f\,f_*$ is nothing else than the joint probability to find at instant t and position x a couple of two particles with respective velocities (v,v_*). Remark that before a collision the two particles are supposed to be uncorrelated, so independent.

One can recognize now in the form of the collision operator (1.4) the five modelling assumptions mentioned above. Indeed, the quadratic nonlinearity of the operator comes from the assumed binary collisions. The fact that the variables (t, x) appear only as parameters comes from the "localized collisions" in space and time. The conservation of momentum and energy (elastic collisions) permits to get the formula (1.3) relating the pre-collisional velocities with the post-collisional ones. The micro-reversibility will be visible in some (symmetry) properties of the collisional kernel b and finally the consequence of the molecular chaos assumption is that the joint probability of finding particles of velocity (v, v_*) before the collision is given by the product form $f\, f_*$.

Taking now into account this type of collisions, the Boltzmann equation reads now

$$\partial_t f + v \cdot \nabla_x f + \frac{F_{ext}}{m} \cdot \nabla_v f = Q(f, f)\,, \tag{1.5}$$

which is a non-linear integro-differential equation, describing the evolution of the density function f of a collisional dilute gas, under the effect of an external force field.

1.2.2 Long range interactions

Besides the just discussed short range interactions, which usually occur in a neutral gas, in a plasma gas long-range interactions are more substantial from a physical point of view. These type of interactions act on longer scales (in time and space) and are due to the existence of the Coulomb or Lorentz forces acting between the charged particles of the plasma gas. These type of interaction will give rise to the **mean field force** term F_{mf} in the Boltzmann equation (1.1), which is somehow an average over all the inter-species interaction forces F_{int}.

To obtain this term, let us simplify here the study and consider a collisionless case, meaning $Q \equiv 0$. In this case one can rigorously obtain the corresponding Vlasov equation from the N particle dynamics (1) by letting $N \to \infty$. Let us give here only the main formal ideas.

Starting from (1) and keeping in mind that we shall consider many particles ($N \to \infty$) in order to pass from the particle (microscopic) description to a more macroscopic desciption of the whole ensemble of particles, we have to adjust the inter-species force term, namely to define

$$F_i := \frac{1}{N} \sum_{k \neq i} F_{int}(x_i - x_k)\,,$$

such that the total force excerced on particle i by the (numerous) other particles is bounded, *i.e.* $F_i = \mathcal{O}(1)$, for $N \to \infty$. This situation is known as the "weak-coupling" scaling. Under such a scaling assumption, the limit $N \to \infty$ is called the **mean-field limit**. Formally, remembering the discrete integration rules, one can hope to have

$$F_i \to_{N\to\infty} F_{mf}(t, x_i(t))\,,$$

with

$$F_{mf}(t, x) := \int_{\mathbb{R}^3} F_{int}(x - y)\, n(t, y)\, dy\,, \qquad n(t, y) := \int_{\mathbb{R}^3} f(t, y, w)\, dw\,,$$

where $n(t,x)$ is the particle density function. This leads to the mean-field Vlasov equation

$$\partial_t f + v \cdot \nabla_x f + \frac{F_{ext} + F_{mf}}{m} \cdot \nabla_v f = 0\,,$$

with

$$F_{mf}(t,x) = -\mathfrak{q}\,\nabla_x \phi_{mf}(t,x)\,, \qquad \phi_{mf}(t,x) := \int_{\mathbb{R}^3} \phi_{int}(x-y)\,n(t,y)\,dy\,.$$

Now, if one considers the Coulomb potential case, given by

$$\phi_{int}(x) := \frac{\mathfrak{q}}{4\pi}\frac{1}{|x|}\,, \quad \text{and leading to} \quad -\Delta\phi_{int} = \mathfrak{q}\,\delta(x)\,,$$

where $\delta(x)$ is the Delta distribution at $x=0$, we deduce

$$-\Delta\phi_{mf}(t,x) = -\int_{\mathbb{R}^3} \Delta\phi_{int}(x-y)\,n(t,y)\,dy = \mathfrak{q}\,n(t,x)\,,$$

such that one gets the coupled Vlasov-Poisson system used in plasma physics to describe the dynamics of a collisionless plasma gas, in the absence of a magnetic field ($B \equiv 0$),

$$\left\{ \begin{array}{l} \partial_t f + v \cdot \nabla_x f + \dfrac{F_{ext} + F_{mf}(t,x)}{m} \cdot \nabla_v f = 0\,, \\ -\Delta\phi_{mf} = \mathfrak{q}\,n(t,x)\,, \qquad F_{mf}(t,x) = -\mathfrak{q}\,\nabla\phi_{mf}\,. \end{array} \right. \tag{1.6}$$

1.3 Properties of the Boltzmann collision operator

Let us now study in more details the Boltzmann collision operator, in particular analyze its specific properties as for example the conservation laws and the entropy decay. Remark that the collision properties assumed at the microscopic level shall be transcribed in some manner at the macroscopic level.
In the following we shall assume that the collisional kernel b satisfies some symmetry properties and that it is furthermore locally integrable, *i.e.*

$$b \in L^1_{loc}(\mathbb{R}^3 \times \mathbb{S}^2)\,, \quad b(v-v_*,\sigma) = b(v_*-v,\sigma)\,, \quad b(v'-v'_*,\sigma) = b(v-v_*,\sigma)\,,$$

for all $v, v_* \in \mathbb{R}^3$ and $\sigma \in \mathbb{S}^2$. Furthermore let us recall that the collision operator acts only on the velocity variable, such that we omitted in this subsection (for simplicity reasons) the parameters (t,x). Then one can show that for any arbitrary and sufficiently smooth function ϕ, we have

$$\int_{\mathbb{R}^3} Q(f,f)(v)\,\phi(v)\,dv = \frac{1}{4}\int\int\int_{\mathbb{R}^3\times\mathbb{R}^3\times\mathbb{S}^2} b(v-v_*,\sigma)\,(f'\,f'_*-f\,f_*)\,(\phi+\phi_*-\phi'-\phi'_*)\,dv\,dv_*\,d\sigma\,.$$

Using now this essential equality permits to show the following properties of the collision operator

Proposition 1.3.1 *(Properties of the Boltzmann collision operator Q)*
For each positive function $f \in C_0(\mathbb{R}^3)$ and each $\phi \in C(\mathbb{R}^3)$ one has the following properties :
(i) Conservation of mass, momentum and energy :

$$\int_{\mathbb{R}^3} Q(f,f)(v)\,\phi(v)\,dv = 0\,, \quad \textit{for} \quad \phi(v) = 1\,,\ v \textit{ or } |v|^2/2\,.$$

(ii) Entropy decay :

$$\begin{aligned} D(f) &:= -\int_{\mathbb{R}^3} Q(f,f)(v)\,\ln(f)\,dv \\ &= \frac{1}{4}\int\int\int_{\mathbb{R}^3\times\mathbb{R}^3\times\mathbb{S}^2} b(v-v-*,\sigma)\,(f'\,f'_* - f\,f_*)\,\ln\left(\frac{f'\,f'_*}{f\,f_*}\right)\,dv\,dv_*\,d\sigma \geq 0\,. \end{aligned}$$

(iii) Thermodynamic equilibrium : The following items are equivalent
- ⊛ $\int_{\mathbb{R}^3} Q(f,f)(v)\,\ln(f)\,dv = 0$ *;*
- ⊛ $Q(f,f)(v) = 0$ *for all* $v \in \mathbb{R}^3$ *;*
- ⊛ f *is a Maxwellian, meaning there exists* $n, T > 0$ *as well as* $u \in \mathbb{R}^3$ *such that*

$$f(v) = \mathcal{M}_{n,u,T}(v) = \frac{n}{(2\pi\,T)^{3/2}}\,e^{\frac{-|v-u|^2}{2\,T}}\,, \quad \forall v \in \mathbb{R}^3\,.$$

These properties are essential in deriving the macroscopic (hydrodynamic) equations from the underlying kinetic model (1.1). Let us comment a little bit more on them.
The word *entropy* stands for a physical quantity associated with a system and describing the tendency of this system to relax towards an equilibrium. It is strongly related with the *irreversibility* of an evolution and the *second law of thermodynamics*, which states that in an isolated system the entropy can never decrease. Boltzmann introduced a mathematical definition of the entropy of a kinetic system described by the distribution function f, by the formula

$$S := -\int_{\mathbb{R}^3}\int_{\mathbb{R}^3} f\,\ln(f)\,dxdv\,.$$

The Boltzmann *H-theorem* states now, that for a gas, governed by Boltzmann's equation (1.1), the H-functional $H := -S$ is nonincreasing in time, namely

$$\frac{d}{dt}H(t) = -\int_{\mathbb{R}^3} D(f)\,dx \leq 0 \qquad \text{and} \qquad \frac{d}{dt}H(t) = 0 \iff f = \mathcal{M}_{n,u,T}\,.$$

The distribution function for whom the entropy remains constant are the so-called *Maxwellians* and are the local thermodynamic equilibria of the considered kinetic system. As the proposition 1.3.1 shows, these distribution functions are those which cancel out the collision operator.

1.4 Other collision operators

In the following we shall present some other basic collision models, that are often used to describe short-range interactions in a neutral gas or in a plasma. A wide variety

of other collision operators exists in literature, adapted for specific situations and other types of particle systems (cells, opinions, birds, *etc*).

BGK-operator :
The Bhatnagar-Gross-Krook (BGK) type operators are very simple artificial operators, used to simplify the Boltzmann model, however which are rather far from physics. If one knows the form of the thermodynamic equilibrium f_{eq} of a particle system, then the BGK-operator constrains the particle distribution function f to tend towards this equilibrium in the long-time asymptotics. In particular it has the form

$$Q_{BGK}(f) = \nu \, (f_{eq} - f) \, , \tag{1.7}$$

where ν is the collisional frequency. In most cases, f_{eq} is a Maxwellian $\mathcal{M}_{n,u,T}$ with (n, u, T) being the moments of the distribution function f. Thus, the BGK-operator is a sort of relaxation operator towards the desired equilibrium state, which conserves the mass, momentum and energy of the system and satisfies the H-theorem. From a mathematical and numerical point of view, the study of the BGK-equation is simpler than the study of the Boltzmann equation. However, the BGK-model is problematic from a physical point of view, as it does not describe adequately all the physical properties of the system, as for example the rate with which the system tends towards the thermodynamic equilibrium.

Fokker-Planck-Landau operator :
The Fokker-Planck-Landau (FPL) collision operator is an approximation of the Boltzmann collision operator, when the collisions become grazing, meaning the deflection of the particles after the "collision" is small. The FPL-operator is particularly useful in plasma physics, where charged particles interact via Coulomb's potential, whereas the Boltzmann operator is more adequate for neutral gases, where the interactions are of hard-sphere type.

The FPL operator has the form

$$Q_{FPL}(f) := \eta \, \nabla_v \cdot \int_{\mathbb{R}^3} \Phi(v - v_*) \, [f(v_*) \, \nabla_v f(v) - f(v) \, \nabla_{v_*} f(v_*)] \, dv_* \, , \tag{1.8}$$

with $\eta = \frac{e^4 \, \ln \Lambda}{8\pi \, \varepsilon_0^2 \, m^2}$ a constant and the semi-positive definite matrix $\Phi(z)$ defined by

$$\Phi(z) := \frac{1}{|z|} \left(Id - \frac{z \otimes z}{|z|^2} \right) .$$

Similar to the Boltzmann operator, it preserves mass, momentum and energy, and dissipates moreover also the entropy. One can rewrite this operator under a parabolic form, the so-called Rosenbluth form, which writes

$$Q_{FP}(f) = \eta \, \nabla_v \cdot [A_\Phi(f) \, f + D_\Phi(f) \, \nabla_v f] \tag{1.9}$$

where A_Φ and D_Φ are given by

$$A_\Phi(f) := -(\nabla \cdot \Phi) * f \, , \qquad D_\Phi(f) := \Phi * f \, .$$

Using this form, the FPL operator can be simplified and gives rise to the differential form of the FPL operator, also called sometimes Fokker-Planck-Kolmogorov operator, of the form

$$Q_{FPK}(f) = \eta \nabla_v \cdot \left[(v-u)f + \frac{k_B T}{m} \nabla_v f \right] , \tag{1.10}$$

where (n, u, T) are the local moments of f. This is done by assuming a Maxwellian molecules cross-section and a distribution function which is radially symmetric. One observes now clearly the action of such an operator, namely the particles are subject to a stochastic diffusion (in the velocity variable) and a determinsitic drift. Indeed, the form (1.10) is a drift-diffusion form.

Linearized operator :
Under the right circumstances it is possible to simplify the collision operators. For example, if we are close to a thermodynamic equilibrium $f_{eq} := \mathcal{M}_{eq}$, it is common to write the distribution function f under the perturbative form

$$f = \mathcal{M}_{eq} + g \, ,$$

with g a small perturbation (in some sense), and to define the linear operator as $\mathcal{L}(g) := Q(\mathcal{M}_{eq} + g, \mathcal{M}_{eq} + g) - Q(g, g)$, meaning we drop the small non-linear terms from the full collision operator. This gives rise to the linearized form of the Boltzmann collision operator

$$\mathcal{L}(g)(t,x,v) := \int_{\mathbb{R}^3} \int_{\mathbb{S}^{d-1}} b(v - v_*, \sigma) \left(\mathcal{M}'_{eq} \, g'_* - \mathcal{M}_{eq} \, g' \right) d\sigma \, dv_* \, .$$

Inelastic collision operator :
Inelastic processes can occur during the plasma evolution, and have thus to be taken into account with an adequate operator. Such processes are for example the recombination of an electron (accompagned with an energy release), the excitation of an electron (through an energy input via vibrations for ex.) and so on. Briefly inelastic proceses are those in which the energy of the particle system is no more conserved, for example taken away from the system in the form of heat. We shall not detail here this type of operators.

1.5 Kinetic-fluid transition

Let us finally detail in this last section the connections between the kinetic theory and the macroscopic fluid theory. We shall focus on different scalings, which shall permit to obtain (formally or rigorously) via an asymptotic limit (usually collisional and long-time limits) the hydrodynamic and the drift-diffusion macroscopic models. An important aim of this asymptotic limit is to establish (formally or even rigorously if possible) the closure relations (as for. ex. (10)) needed to close the fluid model.

Let us thus start with the kinetic model

$$\partial_t f + v \cdot \nabla_x f + \frac{\mathfrak{q}}{m} E \cdot \nabla_v f = Q(f, f) \, , \tag{1.11}$$

where we shall keep in this section the collision operator in an abstract form, satisfying only the usual properties. The connection between the kinetic and the fluid theory will be based on the following ingredients :

— an adequate scaling, permitting to introduce a small parameter $\varepsilon \in (0,1)$ underlying the strength of each term in the kinetic equation. The macroscopic equations are obtained if the gas becomes dense enough, such that the particles undergo many collisions over the time scales of interest ;
— conservation properties of the collision operator, permitting to derive the macroscopic fluid equations ;
— entropy dissipation property of the collision operator, permitting to find the form of the thermodynamic equilibrium and to close the fluid system.

We start by identifying the regimes of interest and the small parameter $\varepsilon \in (0,1)$, characterizing the microscopic/macroscopic description levels of the fusion plasma dynamics and permitting to perform the kinetic-fluid transition. This shall be done in several steps :

1*st* **Step.** *Choice of the characteristic scales* :
We start by firstly introducing the orders of magnitude of the quantities involved in the description of the physical phenomenon we are interested in, as summarized here :

— Macroscopic time and space scale

$$\bar{t} \quad \text{(observation time)}\,, \quad \bar{x} \quad \text{(distance of interest)}\,.$$

— Temperature and electric field

$$\bar{T} \quad \text{(characteristic temperature)}\,, \qquad \mathfrak{q}\,\bar{\phi} = k_B \bar{T}\,, \quad \bar{E} := \frac{\bar{\phi}}{\bar{x}}\,.$$

— Microscopic velocity scale (thermal velocity)

$$\bar{v} := v_{th} = \sqrt{\frac{k_B \bar{T}}{m}}\,.$$

— Microscopic time and length scale, related to the collisional process

$$\tau_c \quad \text{(elapsed time between 2 collisions)}\,,$$
$$l_c := \bar{v}\,\tau_c \quad \text{(mean free path between 2 collisions)}\,.$$

— Collision operators, collisional frequencies, distribution functions

$$\bar{Q} := \frac{\bar{f}}{\tau_c}\,.$$

2*nd* **Step.** *Change of variables* :
With the just defined characteristic scales, we shall perform now the following changes of variables

$$x = \bar{x}x'\,, \quad t = \bar{t}t'\,, \quad v = \bar{v}v'\,, \quad f(t,x,v) = \bar{f}\,f'(t',x',v')\,, \quad etc\,,$$

which lead to the non-dimensional system

$$\partial_{t'} f' + \frac{\bar{v}\,\bar{t}}{\bar{x}}\, v' \cdot \nabla_{x'} f' + \frac{\mathfrak{q}\bar{E}\,\bar{t}}{m\bar{v}}\, E' \cdot \nabla_{v'} f' = \frac{\bar{Q}\,\bar{t}}{\bar{f}}\, Q'(f', f')\,, \tag{1.12}$$

which, using the different relations between the characteristic scales, yields

$$\partial_{t'} f' + \frac{l_c}{\bar{x}}\,\frac{\bar{t}}{\tau_c}\, v' \cdot \nabla_{x'} f' + \frac{l_c}{\bar{x}}\,\frac{\bar{t}}{\tau_c}\, E' \cdot \nabla_{v'} f' = \frac{\bar{t}}{\tau_c}\, Q'(f', f')\,. \tag{1.13}$$

3*rd* **Step.** *Identification of the regime of interest* :
The next step is to characterize the regime of interest. The main assumption for the obtention of macroscopic models is a regime of strong collisionality, defined by the dimensionless Knudsen number

$$\varepsilon := \frac{l_c}{\bar{x}} \ll 1\,.$$

This parameter measures somehow the degree of rarefaction of a gas or its collisionality, as it compares the mean free path of the particles with the typical observation length. It governs the transition from the kinetic theory to the fluid theory. Apart the magnitude of the Knudsen number, we shall also precise the scale of our observational time $\bar{t}$ as compared to the collisional time. This leads to two different macroscopic regimes.

Hydrodynamic regime :
The hydrodynamic regime corresponds to assuming that the considered time-scale is much larger than the collisional time-scale, namely

$$\bar{t} = \frac{\tau_c}{\varepsilon} \gg \tau_c\,,$$

which leads to the singularly-perturbed kinetic equation (the primes were omitted for simplicity reasons)

$$\partial_t f^\varepsilon + v \cdot \nabla_x f^\varepsilon + E \cdot \nabla_v f^\varepsilon = \frac{1}{\varepsilon}\, Q(f^\varepsilon, f^\varepsilon)\,. \tag{1.14}$$

This scaling translates well the fact that scattering is dominant.

Drift-Diffusion regime :
The drift-diffusion regime corresponds to a time-scale even larger than the hydrodynamic time-scale, *i.e.*

$$\bar{t} = \frac{\tau_c}{\varepsilon^2} \gg \tau_c\,,$$

leading to the singularly-perturbed kinetic equation

$$\partial_t f^\varepsilon + \frac{1}{\varepsilon}\, v \cdot \nabla_x f^\varepsilon + \frac{1}{\varepsilon}\, E \cdot \nabla_v f^\varepsilon = \frac{1}{\varepsilon^2}\, Q(f^\varepsilon, f^\varepsilon)\,. \tag{1.15}$$

In comparison to (1.14), the drift-diffusion scaling (1.15) combines strong scattering with very long observational times.

4*th* **Step.** *Asymptotic limits* $\varepsilon \to 0$:
Apart the just performed scaling procedure, the choice of the collisional operator is also very important for getting the asymptotic limit as $\varepsilon \to 0$, in particular getting the desired closure relations. In the limit $\varepsilon \to 0$, the distribution function f^ε gets closer and closer to a Maxwellian (thermodynamic equilibrium) $\mathcal{M}_{n_{eq},u_{eq},T_{eq}}$ dependent on some parameters, as the density $n_{eq}(t,x)$, the mean velocity $u_{eq}(t,x)$ and the temperature $T_{eq}(t,x)$. The evolution of these parameters is provided by some macroscopic fluid equations of the type (6), equations one shall obtain in the limit from kinetic models as (1.14) or (1.15). These thus obtained limit models are the closed macroscopic plasma description models, we are looking for. There are two well-known methods to perform these $\varepsilon \to 0$ asymptotic limits, namely the *Hilbert expansion* method and the *Chapmann-Enskog* method. The aim of Chapter 2 and Chapter 3 will be to study in more details these two kinetic-fluid limits and furthermore to introduce some efficient (Asymptotic-Preserving) schemes, permitting to capture even on the discrete level these asymptotics.

1.6 Some mathematical and numerical difficulties in the study of the kinetic equations

Kinetic equations as the Boltzmann equation or the Fokker-Planck equation are widely used for the description of a lot of applications, like astrophysics, aeronautics, plasma physics, *etc.* Nevertheless, a lot of interesting mathematical problems remain still to be analysed and understood in detail, problems we shall briefly summarize here.

Modelling and microscopic-macroscopic asymptotics :
The validity of the Boltzmann collision operator (or Fokker-Planck operator) poses various problems in some applications (as for. example in highly anisotropic plasma), and new operators to describe an ensemble of (charged) particles are to be introduced. Furthermore, the rigorous mathematical derivation of the Boltzmann equation from fundamental equations, like Newton's laws, is also still an open question. Indeed, the validity of the *Boltzmann-Grad* limit in the collisional case as well as the rigorous justification of the *mean-field* limit in the collisionless case are two important open research fields.

Existence/uniqueness of a solution, regularity, qualitative properties :
Questions related to the existence/uniqueness as well as to the well-posedness of a solution to the Boltzmann equation are still unresolved in general cases. Also the study of the Vlasov-Maxwell system is in its initial phase.

Long-time behaviours :
Starting close to some equilibrium, does the solution remain close to this equilibrium for all times, or even converge towards it or towards another equilibrium ? Such type of questions are not answered for all the kinetic equations. As an example, for the Vlasov-Poisson system, nothing is known about the stability/instability of the BGK-equilibria.

Mesoscopic-macroscopic asymptotics :
For the moment, hydrodynamic limits of the Boltzmann equation permit to obtain the

perfect gas relations, for the fluid closure. How to do, in order to recover other, more realistic closure relations ?

Numerical simulations :
The main goal in computer science is to design numerical schemes which are fast and accurate. Two main problems arise immediately, when trying to solve numerically the Boltzmann equation :

— the non-linearity of the collision operator needs a special treatment ;
— the high-dimensionality of the phase-space ($6D$) leads to enormous computational difficulties.

As one can remark, there remain still a lot of work to do in kinetic theory and the research field is indeed in effervescence. Let us cite here only some of the recent research papers in this field.

— Hydrodynamic limit [21, 27, 28, 32, 33] :

$$\partial_t f + v \cdot \nabla_x f = \frac{1}{\varepsilon} Q(f)\,,$$

where $\varepsilon \ll 1$ stands for the particle mean free path or Knudsen number. This kinetic equation is a diffusive (or collisional) equation and in the limit $\varepsilon \to 0$, one gets the compressible Euler equations.

— Drift-Diffusion scaling [20, 41–43, 47] :

$$\partial_t f + \frac{1}{\varepsilon}(v \cdot \nabla_x f + \nabla_x \Phi \cdot \nabla_v f) = \frac{1}{\varepsilon^2} Q(f)\,,$$

where again $\varepsilon \ll 1$ stands for the Knudsen number. In the diffusive limit $\varepsilon \to 0$, one obtains the Drift-Diffusion model.

— Vlasov-Poisson system in the quasi-neutral limit [5, 23] :

$$\begin{cases} \partial_t f + v \cdot \nabla_x f + \nabla_x \Phi \cdot \nabla_v f = 0 \\ -\lambda^2 \Delta \Phi = 1 - n_e\,, \end{cases}$$

with $\lambda \ll 1$ the rescaled Debye length. The $\lambda \to 0$ limit of this system, is still poorly understood from a mathematical point of view.

— High magnetic field limit [9, 11, 12, 34, 35] :

$$\partial_t f + \frac{1}{\varepsilon} v(p) \cdot \nabla_x f - \frac{1}{\varepsilon}(E + v(p) \times \frac{B}{\varepsilon}) \cdot \nabla_v f = 0\,,$$

where this time $\varepsilon \ll 1$ corresponds to the cyclotronic period. This particular non-collisional kinetic equation is no more diffusive, and the asymptotic behaviour of the solutions f_ε is rather different from the above ones (highly oscillating).

Chapitre 2

Boltzmann equation in the drift-diffusion limit

Chapter based on the articles of :
N. Crouseilles, M. Lemou [1]
M. Lemou and L. Mieussens [2]

In this chapter we shall consider the linear Boltzmann equation in a diffusive scaling $((t,x) \to (t/\varepsilon^2, x/\varepsilon))$, i.e.

$$(P_\varepsilon) \quad \partial_t f + \frac{1}{\varepsilon}\left(v \cdot \nabla_x f + E \cdot \nabla_v f\right) = \frac{1}{\varepsilon^2} Q(f)\,, \quad (x,v) \in \mathbb{R}^3 \times \mathbb{R}^3\,, \ \ t \in \mathbb{R}^+\,. \tag{2.1}$$

This equation describes the state of a gas constituted of ions, evolving in a given electric field E. The distribution function $f(t,x,v)$ stands for the density of the particles located at the position $x \in \mathbb{R}^3$ with velocity $v \in \mathbb{R}^3$ at time $t \geq 0$. The low-density collision operator Q is defined as follows

$$Q(g)(v) := \int \sigma(v,v')\left[M(v)g(v') - M(v')g(v)\right] dv'\,, \tag{2.2}$$

where g belongs to a suitable functional space and M is the Maxwellian distribution function, given by

$$M(v) := \frac{1}{(\pi)^{3/2}} e^{-v^2}\,. \tag{2.3}$$

The cross section σ satisfies the following positivity, boundedness and symmetry (micro-reversibility principle) property

$$0 < \sigma_1 \leq \sigma(v,v') = \sigma(v',v) \leq \sigma_2\,. \tag{2.4}$$

1. "An asymptotic preserving scheme based on a micro-macro decomposition for collisional Vlasov equations : diffusion and high-field scaling limits" , KRM 4 (2011), 441-477.

2. "A new asymptotic preserving scheme based on micro-macro formulation for linear kinetic equations in the diffusion limit", SIAM J. Sci. Comput. 31 (2008), no. 1, 334-368.

The small parameter $0 < \varepsilon \ll 1$ measures the distance of the system to the thermodynamical equilibrium defined by M, and is related to the particle mean free path. In other words, this Boltzmann equation models the dynamics of charged particles, evolving in a given electric field E and a highly collisional framework. It is obtained from a many-body problem under the mean-field approximation. The special linear form of the collision operator is widely used, for example in semiconductor or plasma applications, the model considered here being associated with a linear, low density approximation of the electron-phonon collisions. However, the Asymptotic-Preserving procedure presented in this chapter can be adapted also for other collision operators, as for example the Landau, Fokker-Planck or Boltzmann collision operators.
In the limit $\varepsilon \to 0$, the dominant operator in (2.1) relaxes the system towards an equilibrium state, described by a function belonging to the kernel of Q, the Maxwellian (2.3). The numerical resolution of the Boltzmann equation (2.1) is however rather arduous from a computational point of view, firstly due to its high dimensionality and secondary due to the supplementary difficulty coming from the smallness of ε. Indeed, (2.1) is a singularly perturbed problem and letting formally ε go to zero in (2.1) leads to an ill-posed problem, *i.e.* $Q(f) = 0$. A direct resolution of the Boltzmann equation, via standard schemes, will hence have to cope with this ill-posedness of the problem if ε becomes too small. Refined temporal and spatial grids (dependent on the ε-parameter) are consequently required to allow for an accurate resolution, a procedure which becomes rapidly too costly from a numerical point of view.
Hence, in order to study numerically the asymptotic behaviour of (2.1), one has to try to mimic the asymptotics of the continuous solutions. For this, we will thus firstly investigate the dominant operator and identify the Limit model, when $\varepsilon \to 0$.

2.1 Mathematical framework

Let us keep all over this section the variables (t, x) as fixed (parameters) and consider the Hilbert space

$$\mathcal{H} := L^2(\mathbb{R}^3; M^{-1}(v)\,dv) = \left\{ f \in L^2(\mathbb{R}^3) \ / \ \int_{\mathbb{R}^3} |f(v)|^2 M^{-1}(v)\,dv < \infty \right\} ,$$

associated with the following scalar product

$$(f, g)_{\mathcal{H}} := \int_{\mathbb{R}^3} f(v)\, g(v)\, M^{-1}(v)\, dv\,.$$

Then one can show the following properties of the collision operator Q :

Proposition 2.1.1 *[6,56] Under the assumption (2.4), the collision operator Q, defined by (2.2), satisfies the following properties :*
(i) The linear operator $Q : \mathcal{H} \to \mathcal{H}$ is bounded, symmetric and non-positive.
(ii) The kernel of Q is given by

$$\mathrm{Ker}(Q) := \{\rho M(v) \ / \ \rho \in \mathbb{R}\} \ .$$

(iii) The orthogonal to the kernel of Q is

$$(\mathrm{Ker}(Q))^{\perp} := \left\{ f \in \mathcal{H} \ / \ \int_{\mathbb{R}^3} f(v)\, dv = 0 \right\} .$$

(iv) $-Q$ is coercive on $(\mathrm{Ker}(Q))^{\perp}$, i.e.

$$-\langle Q(f), f \rangle \geq C||f||^2_{\mathcal{H}} , \quad \forall f \in (\mathrm{Ker}(Q))^{\perp} .$$

(v) The range $\mathcal{I}m(Q)$ of Q is closed and coincides with $(\mathrm{Ker}(Q))^{\perp}$. We have moreover the one-to-one mapping

$$Q : (\mathrm{Ker}(Q))^{\perp} \to (\mathrm{Ker}(Q))^{\perp} .$$

Proposition 2.1.2 *Let Π be the mapping defined by*

$$\Pi : \mathcal{H} \to \mathrm{Ker}(Q) , \quad \Pi(f)(v) := \int_{\mathbb{R}^3} f(v')\, dv'\, M(v) = \langle f \rangle\, M(v) , \quad \forall f \in \mathcal{H} . \tag{2.5}$$

Then, we have

$$(f - \Pi(f), g)_{\mathcal{H}} = 0 , \quad \forall f \in \mathcal{H} , \forall g \in \mathrm{Ker}(Q) ,$$

which means that Π is an orthogonal projection on $\mathrm{Ker}(Q)$.

All these properties permit now to identify the limit problem of the Boltzmann equation (2.1) when the perturbation parameter ε tends to zero, which means for vanishing particle mean free path. This limit leads necessary to a macroscopic description of the particle gas. Indeed, inserting the Hilbert-Ansatz

$$f = f_0 + \varepsilon f_1 + \varepsilon^2 f_2 + \cdots$$

in the Boltzmann equation (2.1) and equating the terms of the same order in ε, yields first that $f_0(t, x, \cdot) \in \mathrm{Ker}(Q)$. This means that there exists a density function $\rho_0(t, x)$ such that $f_0 = \rho_0 M$. Moreover, the second equation permits to compute the unique $f_1(t, x, \cdot) \in (\mathrm{Ker}(Q))^{\perp}$ via

$$v \cdot \nabla_x f_0 + E \cdot \nabla_v f_0 = Q(f_1) \quad \Rightarrow f_1 = Q^{-1}(vM) \cdot (\nabla_x \rho_0 - 2\rho_0 E) .$$

The third equation finally yields the limit model (L-model)

$$(L) \ \ \partial_t \rho_0 - \nabla_x \cdot [D(\nabla_x \rho_0 - 2\rho_0 E)] = 0 , \tag{2.6}$$

with the diffusion-matrix given by $D := -\langle v \otimes Q^{-1}(vM) \rangle$. This is the so-called Drift-Diffusion model, describing the evolution of the macroscopic density function ρ_0 in the limit of vanishing mean free path. Remark that the microscale information is contained in this equation in a homogenized way, via the diffusion matrix D.

When the parameter ε is very small, one prefers to solve the macroscopic Drift-Diffusion equation (2.6) instead of (2.1) due to the inherent numerical difficulties detailed in the introduction. However, the DD-model describes well the physics close to the

equilibrium and is thus not suited to describe non equilibrium phenomena. If the mean-free path of the particles ($\sim \varepsilon$) varies within the computational domain, one has to adopt a hybrid strategy in order to get accurate results, solving the Boltzmann equation in regimes where $\varepsilon \sim \mathcal{O}(1)$ and the Drift-Diffusion equation when $\varepsilon \ll 1$. Hybrid strategies are however very laborious from a practical point of view, due to the difficulty to obtain coupling conditions and also to locate the interface between the two regions. The aim of the present chapter is to avoid such a hybrid strategy and to propose a numerical scheme which switches automatically between the Boltzmann and the Drift-Diffusion equations.

2.2 Micro-Macro decomposition

We have seen above that the solution of the kinetic model (2.1) tends, in the limit of vanishing mean free path $\varepsilon \to 0$, towards the solution of a macroscopic model (2.6). Trying to capture this asymptotic behaviour numerically is a very challenging problem. The idea of the construction of such Asymptotic-Preserving schemes is to reformulate the Boltzmann equation in such a manner that it becomes a regular perturbation of the limit problem (2.6).
In more details, the AP-scheme we propose in this chapter is based on a decomposition of the unknown f into a macroscopic part belonging to $\mathrm{Ker}(Q)$ and a microscopic part belonging to $(\mathrm{Ker}(Q))^\perp$. This decomposition is inspired from the fact that in the limit $\varepsilon \to 0$, the solutions f_ε tend towards a function belonging to the kernel of the collision operator, hence inspired from the Hilbert-expansion done above and the obtained Limit-model. A coupled system of equations is then obtained for the micro- respectively macro-components, which degenerates in the limit $\varepsilon \to 0$ towards the Drift-Diffusion limit model.

Let us thus decompose f as follows

$$f = \rho M + \varepsilon G\,, \quad \rho(t,x)M = \Pi(f) \in \mathrm{Ker}(Q)\,, \quad G := \frac{1}{\varepsilon}(f - \Pi(f)) \in (\mathrm{Ker}(Q))^\perp\,.$$

This unique decomposition into an equilibrium and a non-equilibrium part is illustrated in Figure 2.1. Inserting this Ansatz in the kinetic equation (2.1), yields

$$(\partial_t \rho)M + \varepsilon \partial_t G + \frac{1}{\varepsilon}\left(\nabla_x \rho \cdot v M + \varepsilon v \cdot \nabla_x G - 2\rho E \cdot v M + \varepsilon E \cdot \nabla_v G\right) = \frac{1}{\varepsilon} Q(G)\,.$$

Applying now the projection Π on this equation, and performing the subtraction $I - \Pi$ permits to get a micro-macro system for $(\rho M, G)$ (called in the sequel MM-model)

$$(MM) \quad \begin{cases} \partial_t \rho + \nabla_x \cdot \langle vG \rangle = 0 \\ \\ \varepsilon \partial_t G + (I - \Pi)(v \cdot \nabla_x G) + E \cdot \nabla_v G = \dfrac{1}{\varepsilon} Q(G) - \dfrac{1}{\varepsilon}(\nabla_x \rho) \cdot v M + \dfrac{2}{\varepsilon} \rho E \cdot v M\,. \end{cases} \tag{2.7}$$

This formulation is by construction equivalent to the initial equation (2.1). Moreover, in the limit $\varepsilon \to 0$ it permits to get immediately the macroscopic diffusion model, allowing

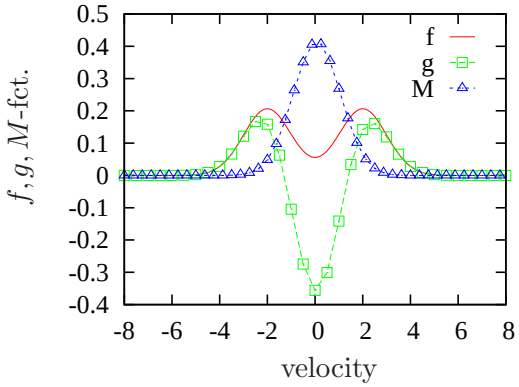

FIGURE 2.1: Micro-macro decomposition of f.

thus for a uniform transition between the kinetic and the macroscopic models. Indeed, one obtains from the second equation, as $\varepsilon \to 0$, that

$$Q(G) = (\nabla_x \rho - 2\rho E) \cdot vM \,,$$

which admits a unique solution $G \in (\mathrm{Ker}(Q))^{\perp}$, as the right hand side belongs to $\mathcal{I}m(Q)$. This solution has the form

$$G = -(\nabla_x \rho - 2\rho E) \cdot \theta \,, \quad \text{where } Q(\theta) = -vM \,, \ \theta \in \left((\mathrm{Ker}(Q))^{\perp}\right)^3 \,.$$

Thus, defining the diffusion coefficient-matrix $D := \langle v \otimes \theta \rangle$, and inserting this G in the first equation of (2.7), yields the $\varepsilon \to 0$ limit model

$$(L) \quad \partial_t \rho - \nabla_x \cdot [D\,(\nabla_x \rho - 2\rho E)] = 0 \,, \tag{2.8}$$

which is exactly the Drift-Diffusion model, we obtained in section 2.1.

To summarize, the micro-macro decomposition of the unknown f, permits to reformulate the singularly perturbed Boltzmann equation (2.1) into an equivalent system (2.7), which is a regular perturbation of the limit problem (2.8). Thus solving numerically (2.7) instead of (2.1) will permit to shift automatically to the limit problem, if the perturbation parameter ε is too small. No temporal or spatial ε-grid-restrictions are any more required to get accurate results, as it would be the case for standard schemes.
This just introduced micro-macro procedure is rather general, and can be simply adapted for a large class of collision operators.

2.3 AP-scheme

To construct an efficient numerical scheme for the resolution of the Boltzmann equation (2.1), we will discretize the equivalent reformulation (2.7) and search for the unknowns $\rho(t,x)$ respectively $G(t,x,v)$. One has to pay attention not to loose, during this discretization-procedure, the AP-property we have established in the continuous case. For simplicity reasons, we will restrict in this chapter the presentation of the AP-scheme to the $1D$ case, the generalisation to multi-D cases being straightforward, but computationally more resource demanding.

2.3.1 Semi-discretization in time

For simplicity, let us introduce a homogeneous discretization of the time-interval $[0,T]$

$$0 = t_0 < \cdots < t_k < \cdots < t_K = T\,; \quad t_k := k\Delta t\,,\ \ k = 0, \cdots, K\,;\ \ K \in \mathbb{N}\,,$$

with the time-step $\Delta t := T/K$. We will denote by $\rho^k(x)$ resp. $G^k(x,v)$ the approximations of $\rho(t_k,x)$ resp. $G(t_k,x,v)$. Then a semi-discretization of (2.7) writes

$$\left\{\begin{array}{l} \dfrac{\rho^{k+1}-\rho^k}{\Delta t} + \nabla_x \cdot \langle v G^{k+1}\rangle = 0\,, \\ \varepsilon\dfrac{G^{k+1}-G^k}{\Delta t} + (I-\Pi)(v\cdot\nabla_x G^k) + E^k\cdot\nabla_v G^k = \dfrac{1}{\varepsilon}Q(G^{k+1}) - \dfrac{1}{\varepsilon}(\nabla_x\rho^k)\cdot vM + \dfrac{2}{\varepsilon}\rho^k E^k\cdot vM\,, \end{array}\right. \tag{2.9}$$

with ρ^0 and G^0 given by the initial conditions. Remark that only the flux in the first equation and the collision term in the second one are taken implicitly. The time-discretization is a hard part in the construction of AP-schemes, in particular the determination of the terms which have to be taken implicitly is arduous and not unique. The important point is that one has to try to implicit only those necessary terms, in order to guarantee the AP-property of the scheme, in particular to recover the correct diffusion limit for $\varepsilon \to 0$. However, the level of implicitness has to be kept low, in order to minimise the computational costs.

Let us now investigate, at least formally, if the just proposed discretization (2.9) tends for $\varepsilon \to 0$ towards a time semi-discretization of the limit model (2.8). Letting thus ε tend to zero in the last equation of (2.9) leads indeed to

$$Q(G^{k+1}) = (\nabla_x\rho^k)\cdot vM - 2\rho^k E^k\cdot vM \quad \Rightarrow \quad G^{k+1} = (\nabla_x\rho^k - 2\rho^k E^k)\cdot Q^{-1}(vM)\,,$$

which, inserted in the first equation, yields indeed a discretization of the limit problem

$$\frac{\rho^{k+1}-\rho^k}{\Delta t} - \nabla_x\cdot\left[D\,(\nabla_x\rho^k - 2\rho^k E^k)\right] = 0\,,$$

with the diffusion matrix again given by $D := -\langle v\otimes Q^{-1}(vM)\rangle$.

2.3.2 Fully discrete system

Let us now introduce a homogeneous discretization of the phase-space interval $[0,L]\times[v_{min},v_{max}]$. Remark that we will consider the macroscopic equation of (2.9) at $x_i := i\Delta x$ for $i = 0,\cdots,N_x$ where $N_x \in \mathbb{N}$ and $\Delta x := L/N_x$ is the space-step. In contrast to this, the microscopic equation of (2.9) will be considered at $x_{i-1/2} := (i-1/2)\Delta x$ for $i = 1,\cdots,N_x$ and at $v_j := v_{min} + j\Delta v$ for $j = 0,\cdots,N_v$ where $N_v \in \mathbb{N}$ and $\Delta v := (v_{max}-v_{min})/N_v$ is the velocity-step. We denote in the sequel by ρ_i^k resp. $G_{i-1/2,j}^k$ the approximations of $\rho(t_k,x_i)$ resp. $G(t_k,x_{i-1/2},v_j)$. Moreover we shall denote by $\rho_{i-1/2}^k := (\rho_i^k+\rho_{i-1}^k)/2$ and evaluate the electric field E at $x_{i-1/2}$, denoting $E_{i-1/2}^k := E(t_k,x_{i-1/2})$. As we are dealing with transport equations, we will use the upwind scheme for the

transport terms and the centred difference scheme for the rest of the terms. Then a phase-space discretization of (2.9) writes : Find $(\rho_i^{k+1}, G_{i-1/2,j}^{k+1})$ solution of

$$\left\{\begin{array}{l} \dfrac{\rho_i^{k+1}-\rho_i^k}{\Delta t} + \left\langle v_j \dfrac{G_{i+1/2,j}^{k+1}-G_{i-1/2,j}^{k+1}}{\Delta x}\right\rangle = 0\,, \quad i=0,\cdots,N_x\,, \\ \varepsilon\dfrac{G_{i-1/2,j}^{k+1}-G_{i-1/2,j}^{k}}{\Delta t} + (I-\Pi)\Phi_{i-1/2,j}^k + \Psi_{i-1/2,j}^k \\ \qquad = \dfrac{1}{\varepsilon}Q_j(G_{i-1/2,\cdot}^{k+1}) - \dfrac{1}{\varepsilon}\left(\dfrac{\rho_i^k-\rho_{i-1}^k}{\Delta x}\right) v_j M_j + \dfrac{2}{\varepsilon}\rho_{i-1/2}^k E_{i-1/2}^k\, v_j M_j\,, \quad i=1,\cdots,N_x\,, \\ \qquad\qquad\qquad\qquad\qquad\qquad\qquad\qquad\qquad\qquad\qquad\qquad j=0,\cdots,N_v\,, \end{array}\right. \tag{2.10}$$

where the fluxes are defined by

$$\Phi_{i-1/2,j}^k := \frac{1}{\Delta x}\left(v_j^+(G_{i-1/2,j}^k - G_{i-3/2,j}^k) + v_j^-(G_{i+1/2,j}^k - G_{i-1/2,j}^k)\right)\,,$$

$$\Psi_{i-1/2,j}^k := \frac{1}{\Delta v}\left(E_{i-1/2}^{k,+}(G_{i-1/2,j}^k - G_{i-1/2,j-1}^k) + E_{i-1/2}^{k,-}(G_{i-1/2,j+1}^k - G_{i-1/2,j}^k)\right)\,,$$

and where we used the notations $v_j^\pm := \frac{v_j \pm |v_j|}{2}$ as well as $E_{i-1/2}^{k,\pm} := \frac{E_{i-1/2}^k \pm |E_{i-1/2}^k|}{2}$. In the discrete case, the bracket $\langle\cdot\rangle$ and the collision operator Q_j are defined by

$$\langle\Theta_j\rangle := \Delta v \sum_{j=0}^{N_v-1}\Theta_j\,, \quad Q_j(g) := \Delta v \sum_{l=0}^{N_v-1}\sigma(v_j,v_l)\left[M(v_j)g_l - M(v_l)g_j\right]\,.$$

Again, let us formally verify that in the limit $\varepsilon\to 0$, we get a discretization of the limit problem (2.8). Putting formally in the microscopic equation $\varepsilon = 0$ yields

$$Q_j(G_{i-1/2,\cdot}^{k+1}) = \left(\frac{\rho_i^k-\rho_{i-1}^k}{\Delta x}\right) v_j M_j - 2\rho_{i-1/2}^k E_{i-1/2}^k\, v_j M_j\,, \ \ \forall j=0,\cdots,N_v$$

which gives

$$G_{i-1/2,j}^{k+1} = \left(\frac{\rho_i^k-\rho_{i-1}^k}{\Delta x} - 2\rho_{i-1/2}^k E_{i-1/2}^k\right) Q_j^{-1}(vM)\,, \ \ \forall j=0,\cdots,N_v\,.$$

Inserting this in the macroscopic equation yields a discretization of (2.8).

2.3.3 Boundary conditions

To solve numerically the Boltzmann equation (2.1), we need a bounded domain and hence realistic boundary conditions. Usually inflow boundary conditions are prescribed for the distribution function f, *i.e.*

$$f(t,0,v) = f_L(v)\,, \quad v>0\,; \qquad f(t,L,v) = f_R(v)\,, \quad v<0\,, \tag{2.11}$$

and $f(t,x,v) = 0$ for all $v \notin (v_{min}, v_{max})$. The problem now is that it is rather hard (or even impossible) to translate the boundary conditions for f in boundary conditions

for the micro-macro unknowns $(\rho(t,x), G(t,x,v))$, which are indispensable for our computations via the developed AP-scheme (2.10). This problem was treated in [20], by introducing artificial boundary conditions, which lead to some unsatisfactory boundary layers, but are more simple to present in the current framework. We will thus expose here this strategy, however, a more realistic approach is proposed in [46], based on a more appropriate micro-macro decomposition, which takes from the beginning better into account for the boundary conditions.

The inflow boundary conditions (2.11) can be rewritten for the micro-macro unknowns as follows

$$\begin{aligned} \rho(t,x_0)M_j + \frac{\varepsilon}{2}\big(G(t,x_{1/2},v_j) + G(t,x_{-1/2},v_j)\big) &= f_L(v_j)\,, \quad \text{if } v_j > 0 \\ \rho(t,x_{N_x})M_j + \frac{\varepsilon}{2}\big(G(t,x_{N_x+1/2},v_j) + G(t,x_{N_x-1/2},v_j)\big) &= f_R(v_j)\,, \quad \text{if } v_j < 0\,. \end{aligned} \tag{2.12}$$

For the other velocities, artificial Neumann boundary conditions are imposed, *i.e.*

$$G(t,x_{-1/2},v_j) = G(t,x_{1/2},v_j)\,, \quad \text{if } v_j < 0\,; \quad G(t,x_{N_x+1/2},v_j) = G(t,x_{N_x-1/2},v_j)\,, \quad \text{if } v_j > 0\,, \tag{2.13}$$

as well as $G(t,x,v) = 0$ for $v \notin (v_{min}, v_{max})$. This altogether shall permit to get sufficient information from the boundary, in order to solve the system (2.10). Indeed, these formulae permit to compute the remaining "ghost"-points, via

$$\begin{aligned} G^{k+1}_{-1/2,j} &= \tfrac{2}{\varepsilon}(f_{L,j} - \rho_0^{k+1}M_j) - G^{k+1}_{1/2,j} \quad \text{if } v_j > 0\,; \quad G^{k+1}_{-1/2,j} = G^{k+1}_{1/2,j} \quad \text{if } v_j < 0; \\ G^{k+1}_{N_x+1/2,j} &= \tfrac{2}{\varepsilon}(f_{R,j} - \rho_{N_x}^{k+1}M_j) - G^{k+1}_{N_x-1/2,j} \quad \text{if } v_j < 0\,; \quad G^{k+1}_{N_x+1/2,j} = G^{k+1}_{N_x-1/2,j} \quad \text{if } v_j > 0\,. \end{aligned} \tag{2.14}$$

2.4 Numerical results

For a numerical analysis of the Asymptotic-Preserving scheme introduced so far, in particular for a detailed stability and consistency study, with a special regard on the ε-independent error estimates, we refer to [49]. In the present section, we shall only compare, for validation, the numerical results obtained via the AP-scheme in the one-dimensional case ($d = 1$), with those obtained via :

— a time explicit upwind scheme for the original Boltzmann equation (2.1), referred to as the "Vlasov-scheme", and where the discretization step sizes are chosen so that the standard transport CFL condition is satisfied, *i.e.*

$$\Delta t = C\min(\varepsilon\beta_x, \varepsilon\beta_v, \varepsilon^2)\,, \quad \beta_x := \frac{\Delta x}{v_{max}}\,, \quad \beta_v := \frac{\Delta v}{E_{max}}\,.$$

— a standard explicit discretization of the diffusion equation (2.8), referred to as the "LIM-scheme", and where the discretization step sizes are chosen so that the standard diffusion stability condition is satisfied, *i.e.*

$$\Delta t = C\min(\Delta x/E_{max}, \Delta x^2)\,.$$

Remark that the time-step size for the Asymptotic-Preserving MM-scheme is linked to the space-step size as follows [20] :

$$\begin{aligned}\Delta t &= C \min_{\varepsilon} \left(\min[C\varepsilon\beta_x/\max(0;1-C\beta_x/\varepsilon), C\varepsilon\beta_v/\max(0;1-C\beta_v/\varepsilon)]\right)\\ &\leq C\min\left(4(C\beta_x)^2, 4(C\beta_v)^2\right)\,.\end{aligned}$$

This stability condition is a combination between a transport CFL-condition and a diffusion stability condition, and has the essential advantage of being ε-independent. The aim is to present some numerical tests in order to validate the asymptotic-preserving property of the micro-macro scheme. For comparisons in the kinetic regime $\varepsilon \sim \mathcal{O}(1)$ we use the Vlasov-solver described above. As this scheme is no more AP in the diffusion limit $\varepsilon \to 0$, we shall compare for $\varepsilon \ll 1$ the MM-scheme results with those obtained by the DD-model.

We coupled our AP-system with the Poisson equation, to be physically more realistic. The initial conditions for the three models are set to

$$\begin{aligned}&(Vlasov) \quad f_0(x,v) := \frac{1}{\sqrt{2\pi}}\exp^{-v^2/2}(1+\alpha\cos(\kappa x))\,, \quad (x,v)\in[0,2\pi/\kappa]\times[v_{min},v_{max}]\,,\\ &(MM) \quad \rho_0(x) := (1+\alpha\cos(\kappa x))\,, \quad g_0(x,v)=0\,, \quad (x,v)\in[0,2\pi/\kappa]\times[v_{min},v_{max}]\,,\\ &(LIM) \quad \rho_0(x) := (1+\alpha\cos(\kappa x))\,, \quad x\in[0,2\pi/\kappa]\,.\end{aligned}$$

α	0.05	$N_x = N_v$	128
κ	0.5	$-v_{min} = v_{max}$	6
ε	$1, \cdots, 0.01$	σ	1

TABLE 2.1: Parameters used in the numerical simulations.

This test case, corresponds to the Landau damping problem and consists in a small perturbation of a Maxwellian equilibrium distribution function and the re-establishment of this equilibrium (for more details see next chapter).

We are plotting in Figure 2.2 the density $\rho(t,x)$, computed via the Vlasov and the MM-scheme, for a large ε-value. As one can observe, the MM-scheme gives results which are very close to those obtained with the "reference" Vlasov-solver. As ε becomes smaller, the computational time for the Vlasov solver becomes prohibitive, such that we can no more compare the MM-solutions with this reference solution. However, we compared in Figure 2.3 the density-function $\rho(t,x)$, computed via the MM-scheme with the results of the limit diffusion model. As one can see, for small ε-values, the MM-results are in good agreement with the Limit-model results.
To compare we also plot in Figure 2.4 the damping (in time) of the electric field $||E(t)||_{L^2}$, obtained with the three different schemes, i.e. Vlasov, MM and LIM-scheme. As one can observe, for $\varepsilon \ll 1$ the details are no more captured with the MM-scheme, as the plasma oscillations are no more resolved. However, the macroscopic behaviour is well recovered. In other words, the MM-scheme is uniformly stable and accurate along the transition from the kinetic to the macroscopic regimes, in particular it is consistent with the Drift-Diffusion model as $\varepsilon \to 0$.

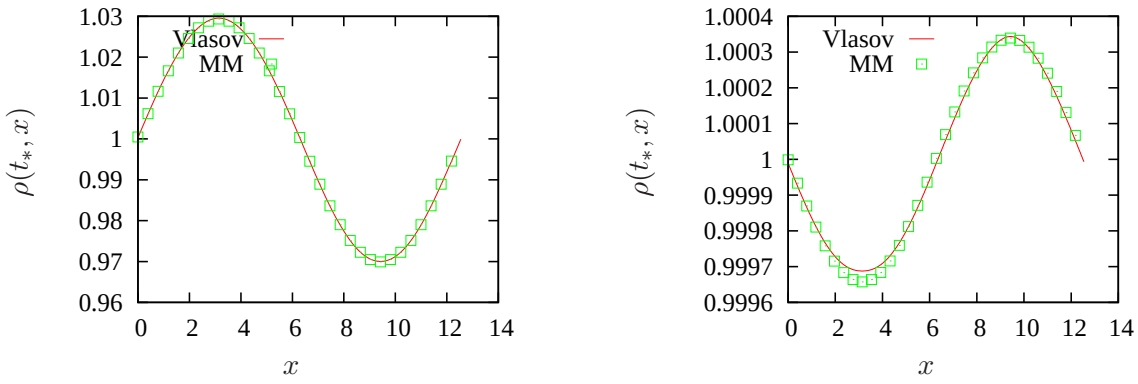

FIGURE 2.2: Density function $\rho(t, x)$ for $t = 1$ and $t = 5$. Perturb. parameter $\varepsilon = 1$

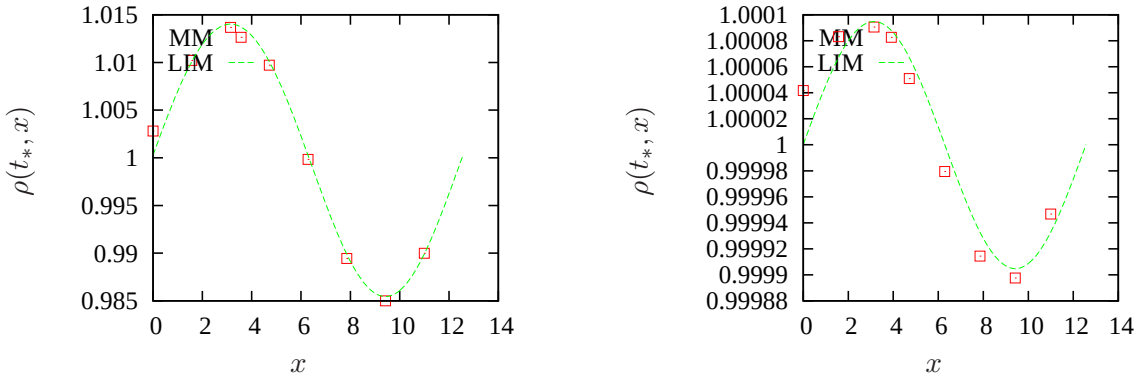

FIGURE 2.3: Density function $\rho(t, x)$ for $t = 1$ and $t = 5$. Perturb. parameter $\varepsilon = 0.01$

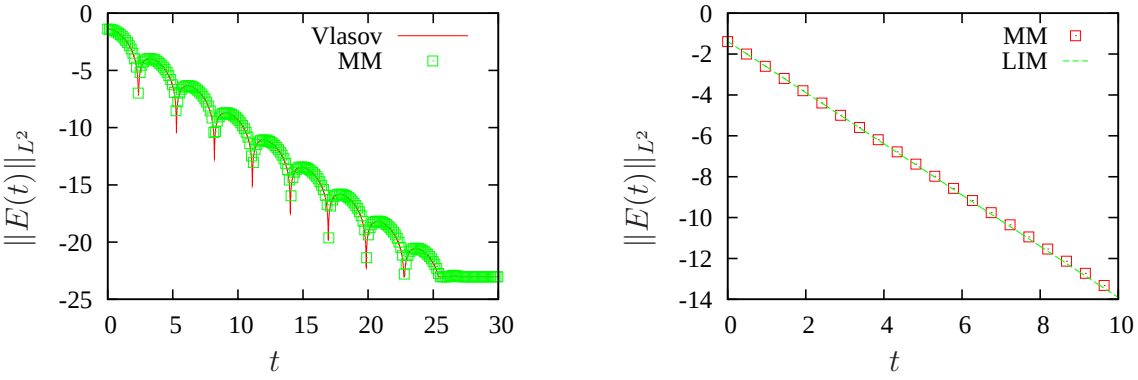

FIGURE 2.4: Linear Landau damping. Electric field evolution $||E(t)||_{L^2}$ (in log scale) for $\varepsilon = 1$ (left) and $\varepsilon = 0.01$ (right).

Chapitre 3

Boltzmann equation in the hydrodynamic limit

Chapter based on the article of :
F. Filbet, S. Jin [1]

In this chapter we are interested in the numerical resolution of the Boltzmann equation in the hydrodynamic regime, meaning close to a thermodynamic equilibrium state. The starting model is the following rescaled electron kinetic equation, obtained in Section 1.5 via an adequate scaling, *i.e.*

$$\partial_t f^\varepsilon + v \cdot \nabla_x f^\varepsilon - E \cdot \nabla_v f^\varepsilon = \frac{1}{\varepsilon} Q(f^\varepsilon, f^\varepsilon)\,, \tag{3.1}$$

with $Q(f,f)$ the Boltzmann collision operator defined in (1.4). When the Knudsen number $\varepsilon \in (0,1)$ is small (ε being the ratio of the mean free path over the typical length scale, and hence a measure of the collisionality or rarefaction of a gas), the collision term becomes stiff, leading to theoretical as well as numerical difficulties. One has to cope then with a singularly-perturbed problem. Using explicit schemes for a numerical resolution of (3.1) necessitates to resolve the small scales incorporated in the problem in order to avoid instability issues. Indeed, a CFL-condition restricts drastically the choice of the time-step Δt, which becomes ε-dependent, leading to enormous computational costs for $\varepsilon \ll 1$. Impliciting the stiff term leads to stable schemes, allowing the use of larger time-steps Δt, however due to the non-linearity and the non-locality of the collision operator $Q(f,f)$, the resolution of (3.1) becomes then a difficult task.
Based on all these reasons, we shall introduce in this chapter an *Asymptotic-Preserving* scheme, founded on an IMEX/BGK-Penalization approach introduced for the first time by [32]. Before presenting this scheme, let us first study the asymptotic behaviour of the solution of (3.1), when the perturbation parameter ε tends towards zero. In particular, a Hilbert expansion method (resp. a Chapman-Enskog method) shall permit us to obtain

1. "A class of asymptotic preserving schemes for kinetic equations and related problems with stiff sources", J. Comp. Physics **229** (2010), no. 20, 7625–7648.

formally the compressible Euler equations (resp. compressible Navier-Stokes equations) in the limit $\varepsilon \to 0$, starting from (3.1). We wish in particular to establish the (perfect gas) closure relations mentioned in the introduction (see (10)), via a clear asymptotic limit starting from the kinetic Boltzmann equation.

3.1 Study of the asymptotic limit $\varepsilon \to 0$

The important step in the study of the asymptotic behaviour of the solution f^ε of (3.1), is a detailed investigation of the specific properties of the dominant operator, here the Boltzmann collision operator introduced in (1.4). In particular, let us recall here its conservation laws and the fundamental entropy decay given in Proposition 1.3.1. Boltzmann's H-theorem is fundamental in the asymptotic study, as it permits to show that in the limit $\varepsilon \to 0$ the distribution function f^ε tends towards a limit function f_0 belonging to the kernel of the collision operator, and hence being a local thermodynamic equilibrium of the form

$$f_0(t,x,v) = \mathcal{M}_{n_0,u_0,T_0} = \frac{n_0}{(2\pi\, T_0)^{3/2}}\, e^{-\frac{|v-u_0|^2}{2\,T_0}}\,, \quad \forall v \in \mathbb{R}^3\,, \tag{3.2}$$

where $\mathcal{M}_{n_0,u_0,T_0}$ stands for the local Maxwellian function, with parameters $n_0(t,x)$, $u_0(t,x)$, $T_0(t,x)$ to be still defined, in order to fully characterize this limit function. The evolution equations permitting to determine these three macroscopic quantities will constitute the asymptotic limit model corresponding to (3.1) when $\varepsilon \to 0$. It is our aim now, to obtain these macroscopic evolution equations.

For this, let us first define the macroscopic quantities corresponding to the distribution function f^ε, like the density $n^\varepsilon(t,x)$, the mean velocity $u^\varepsilon(t,x)$, the temperature $T^\varepsilon(t,x)$ and the total energy $w^\varepsilon(t,x)$, by the formulae

$$n^\varepsilon(t,x) := \int_{\mathbb{R}^3} f^\varepsilon(t,x,v)dv\,, \tag{3.3a}$$

$$n^\varepsilon(t,x)u^\varepsilon(t,x) := \int_{\mathbb{R}^3} v f^\varepsilon(t,x,v)dv\,, \tag{3.3b}$$

$$w^\varepsilon(t,x) := \frac{1}{2}\int_{\mathbb{R}^3} |v|^2 f^\varepsilon(t,x,v)dv = \frac{3}{2}\, n^\varepsilon T^\varepsilon + \frac{1}{2}\, n^\varepsilon |u^\varepsilon|^2\,, \tag{3.3c}$$

$$\frac{3}{2}\, n^\varepsilon(t,x)T^\varepsilon(t,x) := \frac{1}{2}\int_{\mathbb{R}^3} |v-u^\varepsilon|^2 f^\varepsilon(t,x,v)dv\,. \tag{3.3d}$$

Let us also introduce here the pressure tensor and the heat flux

$$\mathbb{P}^\varepsilon(t,x) := \int_{\mathbb{R}^3} (v-u^\varepsilon)\otimes(v-u^\varepsilon) f^\varepsilon(t,x,v)dv\,, \tag{3.4}$$

$$q^\varepsilon(t,x) := \frac{1}{2}\int_{\mathbb{R}^3} |v-u^\varepsilon|^2 (v-u^\varepsilon) f^\varepsilon(t,x,v)dv\,, \tag{3.5}$$

and denote by $p^\varepsilon := n^\varepsilon T^\varepsilon$ the scalar pressure. The (not-closed) fluid model associated to the kinetic equation (3.1) is simply obtained by taking the moments of the Boltzmann-equation and reads

$$\begin{cases} \partial_t n^\varepsilon + \nabla \cdot (n^\varepsilon u^\varepsilon) = 0\,, \\ \partial_t (n^\varepsilon u^\varepsilon) + \nabla \cdot (n^\varepsilon u^\varepsilon \otimes u^\varepsilon) + \nabla \cdot \mathbb{P}^\varepsilon + n^\varepsilon E = 0\,, \\ \partial_t w^\varepsilon + \nabla \cdot (w^\varepsilon u^\varepsilon + \mathbb{P}^\varepsilon \cdot u^\varepsilon) + \nabla \cdot q^\varepsilon + n^\varepsilon E \cdot u^\varepsilon = 0\,. \end{cases} \tag{3.6}$$

This system is not closed, as the pressure tensor and the heat flux $(\mathbb{P}^\varepsilon, q^\varepsilon)$ cannot be (for the moment) related to the other three macroscopic quantities $(n^\varepsilon, u^\varepsilon, w^\varepsilon)$. This is rather natural, as we are still on the microscopic level ($\varepsilon \in (0,1)$ is fixed), such that nothing permits to conclude that we are able to describe the particle gas exclusively via a macroscopic system. However, if we consider that the Knudsen number is small enough, more specifically even that $\varepsilon \to 0$, then we shall be able to close the system. Indeed, as mentioned earlier, in this limit the distribution function f^ε approaches a local thermodynamic equilibrium given by (3.2). Supposing this form, one can then immediately compute the corresponding limit pressure tensor and limit heat flux $(\mathbb{P}_0, q_0)$ via (3.4)-(3.5), to obtain

$$\mathbb{P}_0(t,x) = p_0(t,x)\, Id\,, \qquad p_0(t,x) = n_0\, T_0\,, \qquad q_0 \equiv 0\,. \tag{3.7}$$

These are the so-called perfect gas closure relations. Passing ultimately formally to the limit in (3.6), yields the compressible Euler equations

$$\begin{cases} \partial_t n_0 + \nabla \cdot (n_0 u_0) = 0\,, \\ \partial_t (n_0 u_0) + \nabla \cdot (n_0 u_0 \otimes u_0) + \nabla p_0 + n_0\, E = 0\,, \\ \partial_t w_0 + \nabla \cdot (w_0\, u_0 + n_0\, T_0\, u_0) + n_0 E \cdot u_0 = 0\,, \end{cases} \tag{3.8}$$

which is a well-posed system, permitting the computation of the three macroscopic quantities (n_0, u_0, T_0) which characterize the limit distribution function (3.2) of the Boltzmann equation (3.1).

Finally let us remark that for small but non-zero Knudsen numbers, one can go beyond the leading order term in the perturbation expansion in ε to add correction terms of order $\mathcal{O}(\varepsilon)$ to the limit model (3.8), leading thus to the Navier-Stokes system. Indeed, if one expands the distribution function in a series in ε of the form

$$f^\varepsilon = f_0 + \varepsilon\, f_1 + \varepsilon^2\, f_2 \cdots\,, \tag{3.9}$$

series known as the so-called *Hilbert Ansatz*, then the first term f_0 is the thermodynamic equilibrium found previously. If $\varepsilon \ll 1$ is small but non-zero, one could ask to have some information about the first order term f_1 in order to approximate f^ε more precisely. To obtain such information, we plug the Ansatz (3.9) into the starting kinetic equation (3.1) and compare the terms of the same order in ε. This gives rise to a hierarchy of kinetic equations to be solved to obtain step by step the distribution functions f_1, f_2 $\cdots$. After

some lengthy manipulations (to be found in [22]), one obtains finally the Navier-Stokes system

$$\begin{cases} \partial_t n^\varepsilon + \nabla \cdot (n^\varepsilon u^\varepsilon) = 0\,, \\ \partial_t (n^\varepsilon u^\varepsilon) + \nabla \cdot (n^\varepsilon u^\varepsilon \otimes u^\varepsilon) + \nabla p^\varepsilon + n^\varepsilon\, E = \varepsilon\, \nabla \cdot [\mu_\varepsilon\, \sigma(u^\varepsilon)]\,, \\ \partial_t w^\varepsilon + \nabla \cdot (w^\varepsilon\, u^\varepsilon + p^\varepsilon\, u^\varepsilon) + n^\varepsilon E \cdot u^\varepsilon = \varepsilon\, \nabla \cdot [\mu_\varepsilon\, \sigma(u^\varepsilon)\, u^\varepsilon + \kappa_\varepsilon\, \nabla T^\varepsilon]\,, \end{cases} \tag{3.10}$$

where this time $(n^\varepsilon, u^\varepsilon, w^\varepsilon)$ do not correspond to the full distribution function f^ε but to the truncated one, *i.e.* $f^\varepsilon \sim f_0 + \varepsilon\, f_1$. In this formulation, the static pressure has the form $p^\varepsilon = n^\varepsilon\, T^\varepsilon$ and the rate-of-stress tensor is given by the formula

$$\sigma(u^\varepsilon) := \nabla u^\varepsilon + (\nabla u^\varepsilon)^t - \frac{2}{3}\,(\nabla \cdot u^\varepsilon)\, Id\,. \tag{3.11}$$

If the collision term is a BGK-operator, then the viscosity coefficient has the form $\mu_\varepsilon = \frac{1}{\nu}\, n^\varepsilon\, T^\varepsilon$ and the thermal conductivity is $\kappa_\varepsilon = \frac{5}{2}\, \frac{1}{\nu}\, n^\varepsilon\, T^\varepsilon$. We recognize with these terms the constitutive relations (10) mentioned in the introduction.

We shall present here a slightly different approach to obtain (3.10) from (3.1), the so-called *Chapman-Enskog* method, which is based on the expansion

$$f^\varepsilon = f_0^\varepsilon + \varepsilon\, f_1^\varepsilon + \varepsilon^2\, f_2^\varepsilon \cdots\,, \tag{3.12}$$

which is a modification of the Hilbert Ansatz (3.9) in so far that each term f_l^ε may still depend on ε. Moreover, the leading order term is of the form of a Maxwellian $f_0^\varepsilon := \mathcal{M}_{n^\varepsilon, u^\varepsilon, T^\varepsilon}$ with the same moments $(n^\varepsilon, u^\varepsilon, T^\varepsilon)$ as the full distribution function f^ε. To obtain the (first-order) Navier-Stokes correction terms, let us start in the following with the simplified Ansatz

$$f^\varepsilon = \mathcal{M}_{n^\varepsilon, u^\varepsilon, T^\varepsilon} + \varepsilon\, g^\varepsilon\,, \quad \text{with} \quad \int_{\mathbb{R}^3} g^\varepsilon(v)\, \varphi(v)\, dv = 0 \quad \text{for } \varphi = 1,\, v,\, |v|^2\,. \tag{3.13}$$

Plugging this Ansatz into the pressure tensor (3.4) and the heat flux (3.5) yields

$$\begin{aligned} \mathbb{P}^\varepsilon(t,x) &= \int_{\mathbb{R}^3} (v-u^\varepsilon) \otimes (v-u^\varepsilon) \mathcal{M}_{n^\varepsilon, u^\varepsilon, T^\varepsilon}\, dv + \varepsilon \int_{\mathbb{R}^3} (v-u^\varepsilon) \otimes (v-u^\varepsilon)\, g^\varepsilon(t,x,v)\, dv \\ &= n^\varepsilon T^\varepsilon\, Id + \varepsilon \int_{\mathbb{R}^3} v \otimes v\, g^\varepsilon(t,x,v)\, dv\,, \end{aligned}$$

and

$$\begin{aligned} q^\varepsilon(t,x) &= \frac{1}{2} \int_{\mathbb{R}^3} |v-u^\varepsilon|^2 (v-u^\varepsilon) \mathcal{M}_{n^\varepsilon, u^\varepsilon, T^\varepsilon}\, dv + \frac{\varepsilon}{2} \int_{\mathbb{R}^3} |v-u^\varepsilon|^2 (v-u^\varepsilon)\, g^\varepsilon(t,x,v)\, dv \\ &= \frac{\varepsilon}{2} \int_{\mathbb{R}^3} v\, |v|^2\, g^\varepsilon(t,x,v)\, dv - \varepsilon \int_{\mathbb{R}^3} v \otimes v\, g^\varepsilon(t,x,v)\, dv\,. \end{aligned}$$

In order to find the first order corrections terms to the Euler equations, we have only to find the first order terms in ε of $\mathbb{P}^\varepsilon$ and q^ε, namely to compute

$$\int_{\mathbb{R}^3} v\, |v|^2\, g_0(t,x,v)\, dv\,, \qquad \int_{\mathbb{R}^3} v \otimes v\, g_0(t,x,v)\, dv\,, \tag{3.14}$$

and for this some information about g_0 has to be found. For this, we shall assume we are treating with the BGK-collision operator and hence we can write

$$\begin{aligned} g^\varepsilon &= \frac{f^\varepsilon - \mathcal{M}_{n^\varepsilon,u^\varepsilon,T^\varepsilon}}{\varepsilon} = -\frac{1}{\nu\,\varepsilon}\,Q_{BGK}(f^\varepsilon) = -\frac{1}{\nu}\left[\partial_t f^\varepsilon + v\cdot\nabla_x f^\varepsilon - E\cdot\nabla_v f^\varepsilon\right] \\ &= -\frac{1}{\nu}\left[\partial_t \mathcal{M}^\varepsilon + v\cdot\nabla_x \mathcal{M}^\varepsilon - E\cdot\nabla_v \mathcal{M}^\varepsilon\right] - \frac{\varepsilon}{\nu}\left[\partial_t g^\varepsilon + v\cdot\nabla_x g^\varepsilon - E\cdot\nabla_v g^\varepsilon\right]. \end{aligned}$$

Now, as we are searching only some information on g_0 this last equality yields

$$g_0(t,x,v) = -\frac{1}{\nu}\left[\partial_t \mathcal{M}_0 + v\cdot\nabla_x \mathcal{M}_0 - E\cdot\nabla_v \mathcal{M}_0\right],$$

permitting the computation of the two required quantities (3.14) as functions of (n_0, u_0, T_0) and thus closing the macroscopic system system at order one. Indeed, some lengthy computations lead exactly to the Navier-Stokes system (3.10), completed with the relations (3.11).

3.2 An Asymptotic-Preserving scheme for a BGK-collision operator

After having obtained formally the asymptotic limit models as $\varepsilon \to 0$, let us pass to the numerical part. We shall present in this section an IMEX discretization method for the resolution of (3.1) in the case the collision operator is of BGK-type, *i.e.*

$$Q(f^\varepsilon) := \nu\left(\mathcal{M}_{n^\varepsilon,u^\varepsilon,T^\varepsilon} - f^\varepsilon\right),$$

where $\nu > 0$ is the collisional frequency and the macroscopic parameters defining the Maxwellian $(n^\varepsilon, u^\varepsilon, T^\varepsilon)$ are the moments of f^ε defined by (3.3). The aim is to design a robust scheme for (3.1) permitting additionally to solve automatically the Euler equations (3.8) when the Knudsen number ε tends towards zero. The first idea is to implicit the stiff collision term, to avoid stability issues. Despite the fact that this collision operator is still non-linear, its implicit treatment will reveal to be rather simple and efficient, thanks to the special structure of the BGK-operator. The proposed implicit-explicit (IMEX) discretization scheme writes

$$\frac{f^{k+1} - f^k}{\Delta t} + v\cdot\nabla_x f^k - E\cdot\nabla_v f^k = \frac{\nu}{\varepsilon}\left(\mathcal{M}_{n^{k+1},u^{k+1},T^{k+1}} - f^{k+1}\right), \tag{3.15}$$

where f^k is the approximation of $f(t_k,\cdot)$ at time step $t_k := k\,\Delta t$, $k \in \mathbb{N}$, $\Delta t > 0$, idem for n^k, u^k and so on. The computation of $\mathcal{M}_{n^{k+1},u^{k+1},T^{k+1}}$ can be done completely explicit, as detailed now. Indeed, let us suppose f^k known for some $k \in \mathbb{N}$. Taking the moments of the discretized kinetic equation (3.15) and remembering that the Maxwellian has the same moments as the distribution function (conservation properties of the collision operator), yields the three well-known (discretized) macroscopic equations (compare

with (3.6))

$$\begin{cases} \dfrac{n^{k+1}-n^k}{\Delta t} + \nabla\cdot(n^k u^k) = 0\,, \\ \dfrac{n^{k+1}\,u^{k+1}-n^k\,u^k}{\Delta t} + \nabla\cdot(n^k u^k\otimes u^k) + \nabla\cdot\mathbb{P}^k + n^k\,E = 0\,, \\ \dfrac{w^{k+1}-w^k}{\Delta t} + \nabla\cdot(w^k\,u^k + \mathbb{P}^k\cdot u^k) + \nabla\cdot q^k + n^k E\cdot u^k = 0\,, \end{cases} \tag{3.16}$$

system which allows the computation of $(n^{k+1}, u^{k+1}, T^{k+1})$ from the known macroscopic quantities $(n^k, u^k, T^k, \mathbb{P}^k, q^k)$ (see (3.3)-(3.5)). Knowing now the macroscopic quantities at instant t^{k+1} permits to compute the distribution function f^{k+1} via (3.15). Thus, due to the special structure of the BGK-collision operator, one was able to construct a very simple IMEX-scheme, which has even the essential property of being *weakly AP*, as one can conclude from the next proposition.

Proposition 3.2.1 *[32] Let $\{f^k\}_{k\in\mathbb{N}}$ be a sequence of distribution functions obtained via the IMEX-scheme* (3.15)-(3.16) *with initial condition $f^0 := f_{in}$. Then, if $\varepsilon \ll 1$ and if for some $k_* \in \mathbb{N}$ we have $f^{k_*} = \mathcal{M}^{k_*} + \mathcal{O}(\varepsilon)$, we get*

$$f^j = \mathcal{M}_{n^j,u^j,T^j} + \mathcal{O}(\varepsilon)\,, \quad \forall j \geq k_*\,,$$

where the macroscopic quantities (n^j, u^j, T^j) are related to f^j via (3.3).

This proposition shows a weak-AP feature of the IMEX-scheme, as initially the distribution function f_{in} has to be close to the local thermodynamic equilibrium, in oder to remain for all times close to it. It is more interesting to have a stronger AP-property, namely that regardless of the initial condition f_{in}, there exists a $k_* \in \mathbb{N}$ such that for all $j \geq k_*$ one has $f^j = \mathcal{M}^j + \mathcal{O}(\varepsilon)$.
Nevertheless proposition 3.2.1 proves that if the initial data is well-prepared, the scheme captures well the Euler limit, when $\varepsilon \to 0$, in the sense that the distribution function f^ε converges towards the Maxwellian with moments given by the compressible Euler equations. This property can be very beneficial for numerical simulations.

3.3 An IMEX/BGK-penalization scheme

The simple IMEX-procedure proposed in the previous section is no more applicable for general non-linear collision operators, as for example the Boltzmann or Fokker-Planck operators. In this case, we shall adapt the procedure, by introducing a penalization technique. Let us consider the Boltzmann collision operator (1.4) and propose to split this stiff term into the sum of a non-stiff, non-dissipative part and a stiff dissipative part, as follows

$$\frac{Q(f^\varepsilon)}{\varepsilon} = \frac{Q(f^\varepsilon) - \mathcal{P}(f^\varepsilon)}{\varepsilon} + \frac{\mathcal{P}(f^\varepsilon)}{\varepsilon}\,, \tag{3.17}$$

where the penalization operator $\mathcal{P}$ is linear and chosen such that it preserves the equilibria of Q, meaning for a Maxwellian $\mathcal{M}$ to furnish $\mathcal{P}(\mathcal{M}) = 0$, preserves the conservation

laws, *i.e.*

$$\int_{\mathbb{R}^3} \mathcal{P}(f)(v)\,\varphi(v)\,dv = 0 \quad \text{for } \varphi = 1,\, v,\, |v|^2\,.$$

and furthermore it has to be asymptotically close to the original collision operator Q. In order to find an adequate penalization operator, one idea is to develop $Q(f^\varepsilon)$ around the Maxwellian $\mathcal{M}_{n^\varepsilon,u^\varepsilon,T^\varepsilon}$, namely

$$Q(f^\varepsilon) = Q(\mathcal{M}_{n^\varepsilon,u^\varepsilon,T^\varepsilon}) + dQ(\mathcal{M}_{n^\varepsilon,u^\varepsilon,T^\varepsilon})\,(f^\varepsilon - \mathcal{M}_{n^\varepsilon,u^\varepsilon,T^\varepsilon}) + \mathcal{O}(||f^\varepsilon - \mathcal{M}_{n^\varepsilon,u^\varepsilon,T^\varepsilon}||^2)\,,$$

where we recall that $Q(\mathcal{M}_{n^\varepsilon,u^\varepsilon,T^\varepsilon}) = 0$ and $dQ(\mathcal{M}_{n^\varepsilon,u^\varepsilon,T^\varepsilon})$ is the Frechet derivative of Q around the Maxwellian. A good choice could be then to take

$$\mathcal{P}(f^\varepsilon) := dQ(\mathcal{M}_{n^\varepsilon,u^\varepsilon,T^\varepsilon})\,(f^\varepsilon - \mathcal{M}_{n^\varepsilon,u^\varepsilon,T^\varepsilon})\,.$$

A major problem is now the computation of the Frechet derivative. A simpler choice could be thus to take

$$\mathcal{P}(f^\varepsilon) := \beta\,(f^\varepsilon - \mathcal{M}_{n^\varepsilon,u^\varepsilon,T^\varepsilon})\,, \quad \beta \in \mathbb{R}\,, \tag{3.18}$$

with β to be adequately chosen, approximating somehow $dQ(\mathcal{M}_{n^\varepsilon,u^\varepsilon,T^\varepsilon})$, for example

$$\beta^k := \frac{Q(f^k) - Q(f^{k-1})}{f^k - f^{k-1}} \quad \text{or} \quad \beta := \sup_f \left| \frac{Q(f) - Q(\mathcal{M})}{f - \mathcal{M}} \right|\,.$$

Using now the splitting (3.17) one manner to discretize the corresponding stiff kinetic equation (3.1) is to use an IMEX procedure as follows

$$\frac{f^{k+1} - f^k}{\Delta t} + v \cdot \nabla_x f^k - E \cdot \nabla_v f^k = \frac{Q(f^k) - \mathcal{P}(f^k)}{\varepsilon} + \frac{\mathcal{P}(f^{k+1})}{\varepsilon}\,, \tag{3.19}$$

with the penalization operator given by the BGK-operator (3.18). Thus this scheme handels the stiffness by introducing a penalization operator of BGK-type, which is rather simple to implicit and invert, as seen in the previous section. It takes thus advantage of the special properties of the BKG-operator and preserves on the discrete level the asymptotic transition from the microscopic (kinetic) level to the macroscopic (Euler) level as $\varepsilon \to 0$. Indeed, proposition 3.2.1 holds also in this case.

Let us finally remark that this procedure is not restricted to the Boltzmann collision operator, but can be generalized to any stiff term that admits a local equilibrium. The only difficulty is to find an adequate penalization operator, being at the same time close to the original collision operator, however simple to invert.

3.4 Some numerical simulations

To validate the IMEX/BGK-penalization approach presented in Section 3.3, several numerical simulations for the resolution of the Boltzmann equation (3.1) in the hydrodynamic asymptotics ($\varepsilon \ll 1$) have been performed in [32]. In particular the aim was to test the performances of the proposed AP-scheme (3.19) coupled to (3.16) for several

ε-regimes, from the kinetic rarefied gas regimes ($\varepsilon \sim 1$) to the fluid regimes ($\varepsilon \ll 1$). For large ε-values the IMEX/BGK-penalization results, obtaind by discretizing (3.19), (3.16) via a second order Runge-Kutta/finite volume scheme, were compared with a standard explicit second order Runge-Kutta/finite volume method for (3.1), with a deterministic discretization of the collision operator (spectral method). For small ε-values the obtained results where compared with those obtained via a standard discrztization of the macroscopic models, namely Navier-Stokes for $\varepsilon = 10^{-3}$ and Euler for $\varepsilon = 10^{-4}$. The main goal was to show that :

— the AP-method is uniformly accurate and stable with respect to $\varepsilon > 0$;

— the AP-method captures well the macroscopic asymptotics, for $\varepsilon \to 0$.

We shall present here only one test corresponding to the numerical resolution of the Boltzmann equation (3.1) with a Knudsen-parameter ε which is variable in space, as represented in Figure 3.1. This case occurs rather frequently in applications, as the plasma properties, for ex. the rarefaction and hence the collisionality, can be space-dependent, and it is a rather difficult problem to cope with, as different length scales are present at the same time in the problem and have to be treated adequately. In our case, we shall take $\varepsilon : \mathbb{R} \to \mathbb{R}^+$ defined as

$$\varepsilon(x) = \varepsilon_0 + \frac{1}{2}\left[\tanh(1 - 11x) + \tanh(1 + 11x)\right], \quad \varepsilon_0 \in (0, 1)\,.$$

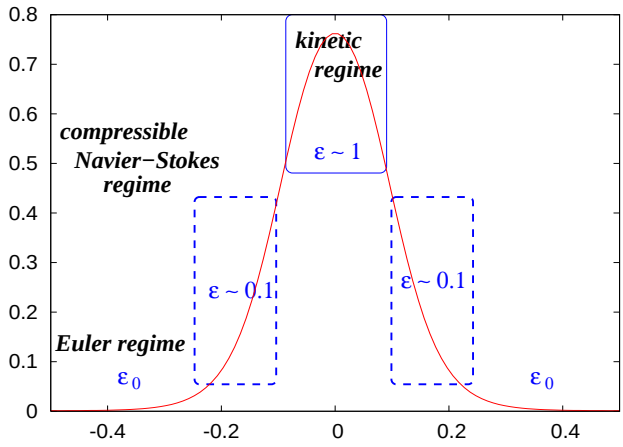

FIGURE 3.1: Different ε-regimes could be present in the problem.

The considered initial condition is chosen to be far from a Maxwellian thermodynamic equilibrium, namley

$$f_{in}(x, v) := \frac{n_0}{2}\left[\exp\left(-\frac{|v - u_0|^2}{T_0}\right) + \exp\left(-\frac{|v + u_0|^2}{T_0}\right)\right], \quad (x, v) \in [-L, L]\times[-v_{max}, v_{max}]^2\,,$$

with $u_0 = (3/4, -3, 4)$ and

$$n_0(x) := \frac{2 + \sin(kx)}{2}, \quad T_0(x) := \frac{5 + 2\cos(kx)}{20},$$

where we shall choose $L = 1/2$, $k = \pi/L$, $v_{max} = 7$ as well as periodic boundary conditions in x and vanishing conditions in velocity. Figures 3.2-3.4 show the comparison of the numerical results obtained with the above mentioned two numerical approaches, the traditional one, as well as the AP IMEX/BGK-penalization method. In order to be able to use a traditional approach, we took $\varepsilon_0 = 10^{-3}$ such that the CFL-condition does not enhance the computation. Indeed, the CFL-condition for standard schemes requires a very restrictive time step $\Delta t \sim \mathcal{O}(\varepsilon)$, leading in the present case to $\Delta t_{stand} = 10^{-4}$ whereas the CFL-condition of the AP-scheme is $\Delta t_{AP} = 10^{-3}$. The difference between these two time-steps becomes more drastic for smaller ε_0-values, such that the traditional approaches can no more be used. One observes now from Figure 3.2-3.4 that the two simulation results are in good agreement, even if the AP-scheme does not resolve all the small time-scale.

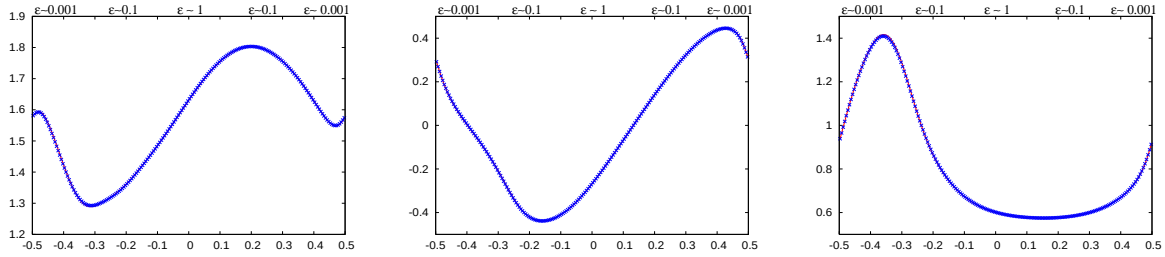

FIGURE 3.2: Comparision of the evolution of $n(t,\cdot)$ (left), $u(t,\cdot)$ (middle) and $T(t,\cdot)$ (right) for $t = 0.25$. The line corresponds to the standard scheme whereas the stars correspond to the AP-scheme.

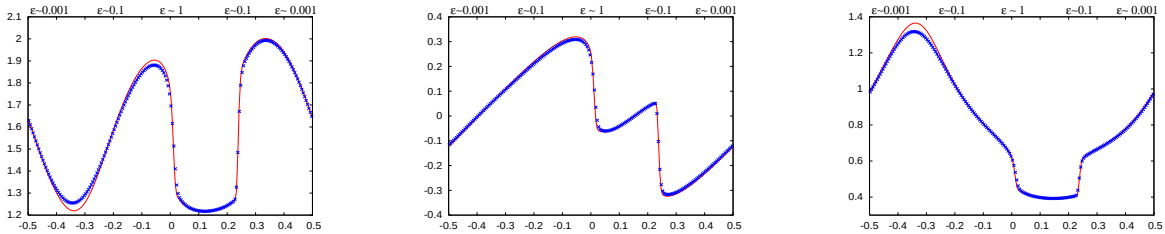

FIGURE 3.3: Same computations for $t = 0.5$.

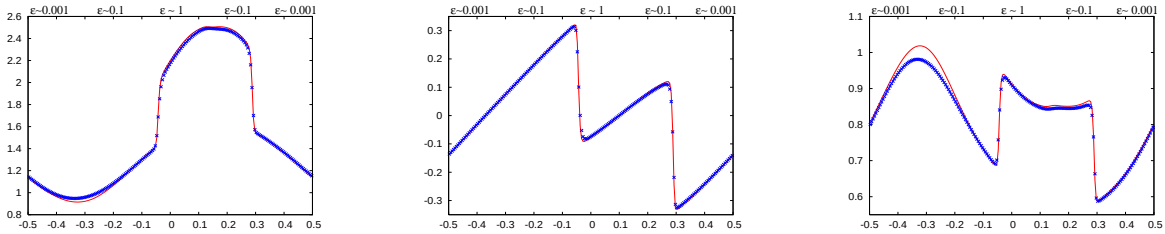

FIGURE 3.4: Same computations for $t = 0.75$.

Chapitre 4

Boltzmann equation in the high-field limit

Chapter based on the article of :
B. Fedele, C. Negulescu, S. Possanner [1]

The objective of this last chapter is to introduce and study an efficient numerical scheme for the resolution of evolution problems containing stiff transport terms, namely

$$\partial_t f^\varepsilon + \mathcal{L} f^\varepsilon + \frac{\mathbf{b}}{\varepsilon} \cdot \nabla f^\varepsilon = 0\,, \quad t \in \mathbb{R}^+\,,\ \mathbf{x} \in \Omega \subset \mathbb{R}^d\,, \tag{4.1}$$

where $\mathbf{b} : \mathbb{R}^+ \times \Omega \to \mathbb{R}^d$ is a known or self-consistently computed vector-field satisfying $\nabla \cdot \mathbf{b} = 0$, and $\mathcal{L}$ is a given operator (for ex. transport or diffusion operator). The small parameter $\varepsilon \ll 1$ represents the stiffness of the problem and signifies that we have to cope with a very strong vector-field $\mathbf{b}$. It brings up the main difficulties in the numerical resolution of (4.1) and this due to the introduction of multiple scales in the problem. Indeed, the dynamics along the $\mathbf{b}$-field is very rapid, as compared to its perpendicular evolution. In the formal limit $\varepsilon \to 0$, the problem reduces to the constraint

$$\mathbf{b} \cdot \nabla f^0 = 0\,, \tag{4.2}$$

which signifies that the unknown f^0 is constant along the field-lines of $\mathbf{b}$. However, in general, problem (4.2) does not permit to determine this constant, for example when $\mathbf{b}$ has closed field lines. Thus the reduced problem (4.2) is ill-posed, information has been lost while setting formally $\varepsilon = 0$ in (4.1). This feature is typical for singularly-perturbed problems and brings a lot of mathematical as well a numerical difficulties into play.

Concerning the numerical simulation of (4.1), standard explicit numerical schemes require very small time steps, dependent on the ε-parameter, in order to accurately

1. "Asymptotic-Preserving scheme for the resolution of evolution equations with stiff transport terms", SIAM MMS (Multiscale Model. Simul.) 17 (2019), no. 1, 307–343.

account for the microscopic information (living at the ε-scale). This procedure, even if accurate, has however the big disadvantage of being numerically very costly in simulation time and memory. Fully implicit schemes or IMEX-schemes are also not of use for $\varepsilon \ll 1$, due to the ill-conditioned limit model. Alternative methodologies are thus required taking into account for the various scales present in the problem. Asymptotic analysis will be one of the mathematical tools used in this chapter, permitting to recover the microscopic information lost in the reduced model (4.2) and to design the numerical scheme presented here.

Evolution equations of the type (4.1) arise often in applications coming from fluid dynamics [52] and plasma physics [17,37,57]). To mention only some examples, in thermonuclear tokamak plasmas, the evolution of ions is described via the non-dimensional Vlasov ($\eta = 0$) or Fokker-Planck ($\eta \neq 0$) equation

$$\partial_t f_i^\epsilon + \mathbf{v} \cdot \nabla_{\mathbf{x}} f_i^\epsilon + \Big(\mathbf{E} + \frac{1}{\varepsilon} \mathbf{v} \times \mathbf{B} \Big) \cdot \nabla_{\mathbf{v}} f_i^\epsilon = \eta \, \nabla_{\mathbf{v}} \cdot [\mathbf{v} f_i^\varepsilon + \nabla_{\mathbf{v}} f_i^\varepsilon] \, , \tag{4.3}$$

where $f_i^\epsilon(t, \mathbf{x}, \mathbf{v})$ represents the ion distribution, dependent on time, space and velocity. This equation is coupled via the electromagnetic fields $(\mathbf{E}(t, \mathbf{x}), \mathbf{B}(t, \mathbf{x}))$ to an equation describing the electron evolution. The coupling is done by means of Maxwell's equations or Poisson equation in the electrostatic case. The magnetic field is very strong in tokamak experiments in the aim to confine the plasma and to render the fusion possible. This feature is translated in (4.3) in the magnitude of the scaling parameter $\varepsilon \ll 1$.

The second example we shall be interested in here, concerns the long-time asymptotic study of the electron $1D1V$ Vlasov-Poisson system

$$\begin{cases} \partial_t f_e + v \, \partial_x f_e - E(t,x) \, \partial_v f_e = 0 \, , \qquad \forall t \in \mathbb{R}^+ \, , \ \ \forall (x,v) \in \Omega \subset \mathbb{R}^2 \\ -\partial_{xx} \varphi = 1 - n_e \, , \qquad n_e(t,x) = \displaystyle\int_{\mathbb{R}} f_e(t,x,v) \, dv \, , \qquad E = -\partial_x \varphi \, . \end{cases} \tag{4.4}$$

Introducing the field $\mathbf{u} := (v, -E(t,x))^t$ and the stream function $\Psi := \frac{1}{2}|v|^2 - \varphi(t,x)$, one has $\mathbf{u} = ^\perp \nabla \Psi$, where $^\perp \nabla := (\partial_v, -\partial_x)$. Considering additionally long-time scales, the Vlasov-Poisson system (4.4) transforms into the nonlinear, coupled system

$$\begin{cases} \partial_t f_e^\varepsilon + \dfrac{\mathbf{u}^\varepsilon}{\varepsilon} \cdot \nabla_{x,v} f_e^\varepsilon = 0 \, , \qquad \forall (t,x,v) \in \mathbb{R}^+ \times \Omega \\ -\Delta_{x,v} \Psi^\varepsilon = n_e^\varepsilon - 2 \, , \qquad n_e^\varepsilon(t,x) = \displaystyle\int_{\mathbb{R}} f_e^\varepsilon(t,x,v) \, dv \, , \qquad \mathbf{u}^\varepsilon = ^\perp \nabla \Psi^\varepsilon \, . \end{cases} \tag{4.5}$$

Finally our last example comes from fluid mechanics : consider the incompressible Euler equations in the long-time scaling, describing a bi-dimensional, inviscid flow with velocity $\mathbf{u} := (u_1, u_2, 0)$ and pressure p

$$\begin{cases} \varepsilon \, \partial_t \mathbf{u}^\varepsilon + (\mathbf{u}^\varepsilon \cdot \nabla) \mathbf{u}^\varepsilon + \nabla p^\varepsilon &= 0 \, , \qquad \forall (t, \mathbf{x}) \in \mathbb{R}^+ \times \Omega \, , \\ \nabla \cdot \mathbf{u}^\varepsilon &= 0 \, . \end{cases} \tag{4.6}$$

Introducing the vorticity $\omega^\varepsilon := \nabla \times \mathbf{u}^\varepsilon$, the Euler system leads to the following nonlinear, coupled system

$$\left\{ \begin{array}{l} \partial_t \omega^\varepsilon + \dfrac{\mathbf{u}^\varepsilon}{\varepsilon} \cdot \nabla \omega^\varepsilon = 0 \,, \\ -\Delta \Psi^\varepsilon = \omega^\varepsilon \,, \qquad \mathbf{u}^\varepsilon = {}^\perp \nabla \Psi^\varepsilon \,, \end{array} \right. \tag{4.7}$$

constituted of a transport equation for the vorticity, which is self-consistently coupled with a Poisson equation for the determination of the stream-function Ψ^ε, result of the divergence-free constraint of $\mathbf{u}^\varepsilon$. Sometimes one can add on the right hand side of the first equation in (4.7) a small viscosity term $\nu \Delta \omega^\varepsilon$, ν being the reciprocal of the Reynolds number. The new modified equation (4.7) is coming then from the incompressible Navier-Stokes equations.

The goal of this chapter is now to present and investigate an efficient, uniformly accurate and stable (wrt. ε) numerical scheme for the resolution of the following linear, stiff transport problem

$$(V)^\varepsilon \quad \left\{ \begin{array}{l} \partial_t f^\varepsilon + \dfrac{\mathbf{b}}{\varepsilon} \cdot \nabla f^\varepsilon = 0 \,, \qquad \forall t \in (0,T) \,, \ \forall \mathbf{x} = (x,y) \in \Omega \subset \mathbb{R}^2 \,, \\ f^\varepsilon(0,\mathbf{x}) = f_{in}(\mathbf{x}) \qquad \forall \mathbf{x} \in \Omega \,, \end{array} \right. \tag{4.8}$$

with given, smooth and time-independent vector-field $\mathbf{b} : \Omega \to \mathbb{R}^2$, satisfying $\nabla \cdot \mathbf{b} = 0$. This simplified transport equation contains all the numerical difficulties arising also in the original equation (4.1). Given an efficient numerical algorithm for the resolution of (4.8), the treatment of the examples mentioned above is straightforward. Indeed, the nonlinear coupling can be treated iteratively and the discretization of the general not-stiff term $\mathcal{L} f^\varepsilon$ of (4.1) can be done via standard schemes suited for this particular operator. The scheme we propose here shall be verified and validated in the long-time asymptotics of the Vlasov-Poisson system (4.5).

Due to the divergence constraint of $\mathbf{b}$, there exists a stream-function Ψ such that $\mathbf{b} = {}^\perp \nabla \Psi$. Using the Poisson-bracket notation for two functions χ, θ, namely

$$\{\chi, \theta\} := \partial_x \chi \, \partial_y \theta - \partial_y \chi \, \partial_x \theta = \nabla \chi \cdot {}^\perp \nabla \theta \,, \tag{4.9}$$

the transport equation (4.8) can be simply rewritten as

$$(V)^\varepsilon \quad \left\{ \begin{array}{l} \partial_t f^\varepsilon + \dfrac{1}{\varepsilon} \{f^\varepsilon, \Psi\} = 0 \,, \quad t \in \mathbb{R}^+ \,, \ \mathbf{x} \in \Omega \subset \mathbb{R}^2 \,, \\ f^\varepsilon(0,\cdot) = f_{in} \,, \end{array} \right. \tag{4.10}$$

and shall be completed with adequate boundary conditions. In order to recover the Vlasov-Poisson test case presented above, we shall assume the following Hypothesis.

Hypothesis A : *The domain Ω will be an infinite strip $(L_1, L_2) \times \mathbb{R}$ of the (x,y)-plane. Furthermore, we shall assume periodic boundary conditions in x and the field $\mathbf{b}$ is supposed to be also periodic in x.*

Our main goal is to understand in detail the features of the Asymptotic-Preserving scheme we intent to propose for the resolution of (4.8). In particular, we aim to :

— design a simple and robust numerical scheme, working on a Cartesian grid ;
— design a scheme which enjoys the Asymptotic-Preserving properties (AP-scheme), in the sense that it has to be uniformly stable and accurate wrt. ε ;
— design a scheme which has to be simply "generalizable" to more dimensions and various advection fields.

4.1 Asymptotic-Preserving reformulation

let us introduce now an AP-reformulation of the singularly-perturbed advection problem (4.8) completed with adequate boundary conditions, explicited in *Hypothesis A*, scheme which shall behave better (regularly) in the limit $\varepsilon \to 0$. For this, the well-posed limit-model has firstly to be identified by investigating the asymptotic behaviour of the solutions f^ε, as $\varepsilon \ll 1$. We underline here that $\mathbf{b}$ is time-independent in the following, if not explicitly mentioned, as in Section 4.2.

4.1.1 Identification of the limit model

As mentioned in the introduction, letting formally $\varepsilon \to 0$ in (4.8), leads to an ill-posed problem, which does not permit to compute in a unique manner the limit solution $f^0(t,x,y)$. The only information we get is that f^0 is constant along the field-lines of $\mathbf{b}$.

In order to establish the limit model $(V)^0$ corresponding to (4.8), let us suppose that f^ε admits the following Hilbert expansion

$$f^\varepsilon = f^0 + \varepsilon f^1 + \varepsilon^2 f^2 + \dots . \tag{4.11}$$

Injecting this Ansatz in (4.8) leads to the infinite hierarchy of equations

$$\begin{aligned} \mathbf{b}\cdot\nabla f^0 &= 0, && (4.12)\\ \partial_t f^0 + \mathbf{b}\cdot\nabla f^1 &= 0, && (4.13)\\ \partial_t f^1 + \mathbf{b}\cdot\nabla f^2 &= 0, && (4.14)\\ &\vdots \end{aligned}$$

Equation (4.12) reveals that f^0 belongs to the kernel of the dominant operator $\mathcal{T} := \mathbf{b}\cdot\nabla$. However, this information is not enough to determine completely f^0. It is necessary to use the next equation (4.13), to get the missing information. To eliminate f^1 from this equation, one projects (4.13) on the kernel of $\mathcal{T}$. This projection is nothing else than the average of a quantity q along the field lines of $\mathbf{b}$ and will be denoted by $\langle q\rangle$. Briefly, if $Z(s;\mathbf{x})$ is the characteristic flow associated to the field $\mathbf{b}$, *i.e.*

$$\begin{cases} \dfrac{d}{ds}Z(s;\mathbf{x}) = \mathbf{b}(Z(s;\mathbf{x}))\,, \\ Z(0;\mathbf{x}) = \mathbf{x}\,, \end{cases}$$

the average of a function $q \in L^2(\Omega)$ over the field lines of $\mathbf{b}$ is defined as

$$\langle q \rangle(\mathbf{x}) := \lim_{S\to\infty} \frac{1}{S} \int_0^S q(Z(s;\mathbf{x}))\, ds \quad \forall \mathbf{x} \in \Omega\,.$$

One can show (after some hypothesis on the regularity of $\mathbf{b}$, see [10]) that $\langle\cdot\rangle$ is a well-defined application, furthermore that $\langle q \rangle$ is constant along the field lines of $\mathbf{b}$ and $\langle \mathbf{b}\cdot\nabla q\rangle = 0$. The above mentioned procedure permits then to obtain a well-posed limit model for f^0. We already know that f^0 belongs to the kernel of $\mathcal{T}$, meaning $f^0 = \langle f^0 \rangle$, such that the limit model $(V)^0$ writes

$$(V)^0 \quad \begin{cases} \partial_t f^0 = 0, \qquad \mathbf{b}\cdot\nabla f^0 = 0\,, \qquad \forall (t,\mathbf{x}) \in (0,T)\times\Omega\,, \\ f^0(0,\mathbf{x}) = \langle f_{in}(\mathbf{x})\rangle \in \ker \mathcal{T}\,, \qquad \mathbf{x}\in\Omega\,. \end{cases} \tag{4.15}$$

The following theorem proves rigorously the convergence of the solution f^ε of (4.8) towards the solution f^0 of the limit model (4.15), as $\varepsilon \to 0$.

Théorème 4.1.1 *[10] Consider a subset Ω of $\mathbb{R}^2$ satisfying Hypothesis A. Assume $\mathbf{b} \in W^{1,\infty}_{loc}(\mathbb{R}^2)$, where we extend $\mathbf{b}$ periodically to the whole $\mathbb{R}^2$, satisfying $\nabla\cdot\mathbf{b} = 0$ as well as the growth condition*

$$\exists C > 0 \;\; s.t. \;\; |\mathbf{b}(\mathbf{x})| \le C\,(1+|\mathbf{x}|)\,, \quad \forall \mathbf{x}\in\Omega\,.$$

Suppose furthermore that $f_{in} \in L^2(\Omega)$. Then (4.8) resp. (4.15) admit unique weak solutions $f^\varepsilon, f^0 \in L^\infty(0,T;L^2(\Omega))$ and one has $f^\varepsilon \underset{\epsilon\to 0}{\overset{\star}{\rightharpoonup}} f^0$, weakly-$\star$ in $L^\infty(0,T;L^2(\Omega))$.
If the initial conditions are well prepared in the sense that f^ε_{in} is smooth enough and satisfies $f^\varepsilon_{in} \underset{\epsilon\to 0}{\to} f^0_{in} \in \ker\mathcal{T}$ in $L^2(\Omega)$, then one has even $f^\varepsilon \underset{\epsilon\to 0}{\to} f^0$ in $L^\infty(0,T;L^2(\Omega))$.

4.1.2 Micro-Macro reformulation

The design of a multiscale numerical procedure for the resolution of problem (4.8) is now inspired by the asymptotic study performed in Section 4.1.1. To recover the missing microscopic information in the reduced model (4.2), we shall decompose f^ε into a macroscopic and a microscopic part, as follows

$$f^\varepsilon = p^\varepsilon + \varepsilon\, q^\varepsilon\,, \quad \text{with } \; \mathbf{b}\cdot\nabla f^\varepsilon = \varepsilon\,\mathbf{b}\cdot\nabla q^\varepsilon\,. \tag{4.16}$$

This signifies that p^ε belongs to the kernel of the dominant operator $\mathcal{T} = \mathbf{b}\cdot\nabla$ and is considered as the macroscopic part. This decomposition is not unique as one has still to fix the values of p^ε or equivalently of q^ε on the field-lines, fact which shall be done in the next subsections.
Plugging for the moment (4.16) into (4.8) leads to the following augmented system for the two unknowns $(f^\varepsilon, q^\varepsilon)$

$$\begin{cases} \partial_t f^\varepsilon + \mathbf{b}\cdot\nabla q^\varepsilon = 0\,, \qquad \forall (t,\mathbf{x}) \in (0,T)\times\Omega\,, \\ \mathbf{b}\cdot\nabla f^\varepsilon = \varepsilon\,\mathbf{b}\cdot\nabla q^\varepsilon\,, \qquad \forall (t,\mathbf{x}) \in (0,T)\times\Omega\,, \end{cases} \tag{4.17}$$

associated with the initial condition $f^\varepsilon(0,\cdot) = f_{in}$ and adequate boundary conditions (*Hypothesis A*). Now several possibilities are conceivable to fix the values of q^ε on the

field-lines, fact which is nothing else than rendering the decomposition (4.16) unique. Let us observe here that the values of q^ε on these lines are of no importance for the computation of our physical unknown f^ε, as only $\mathbf{b}\cdot\nabla q^\varepsilon$ is occurring in the system (4.17). Thus any arbitrary choice could do the work.

4.1.3 Zero mean value

From a purely mathematical point of view, one first idea is to fix the average of q^ε along the field lines of $\mathbf{b}$, by enforcing zero mean, *i.e.*

$$\langle q^\varepsilon \rangle = 0\,. \tag{4.18}$$

Imposing (4.18) can be done by slightly changing the system, adding an additional "subtle" term, with $\sigma \in \mathbb{R}$ an arbitrary constant, namely

$$\left\{ \begin{array}{l} \partial_t f^\varepsilon + \mathbf{b}\cdot\nabla q^\varepsilon = 0\,, \\ \mathbf{b}\cdot\nabla f^\varepsilon = \varepsilon\,\mathbf{b}\cdot\nabla q^\varepsilon - \sigma\,\langle q^\varepsilon\rangle\,. \end{array} \right. \tag{4.19}$$

Indeed, one can remark immediately that taking the average of the second equation over the field-lines automatically yields the constraint $\langle q^\varepsilon\rangle = 0$. The new introduced term is hence a tricky zero, rendering q^ε unique by fixing its average values along the $\mathbf{b}$-lines to zero. One can show now that (4.19) is completely equivalent to (4.8), for each $\varepsilon > 0$. Indeed, two ingredients help to prove this equivalence between both formulations. On one hand, for given f^ε and $\varepsilon > 0$, the equation

$$\left\{ \begin{array}{l} \mathbf{b}\cdot\nabla q^\varepsilon = \dfrac{1}{\varepsilon}\mathbf{b}\cdot\nabla f^\varepsilon, \\ \langle q^\varepsilon\rangle = 0\,, \end{array} \right.$$

has a unique solution q^ε. On the other hand, the second equation in (4.19) yields immediately, as mentioned above, the constraint $\langle q^\varepsilon\rangle = 0$.

This idea is very nice from a mathematical point of view, however, if one is thinking at the numerical implementation, one has to average over the field lines of $\mathbf{b}$, in order to discretize the new term $\sigma\,\langle q^\varepsilon\rangle$ in the second equation of (4.19). This procedure is rather hard (we are working on Cartesian grids with not-aligned fields $\mathbf{b}$) and can introduce moreover ε-dependent error terms in the results. Thus we shall leave this idea behind, and search for a more practical one.

4.1.4 The AP-reformulation

In order to render q^ϵ unique in (4.17), one can imagine to use a regularization technique. Regularization is a very broad field in mathematics, and is devoted to the design and analysis of methods for obtaining stable solutions of ill-posed problems. In particular, the usual regularization technique consists in replacing the ill-posed problem by a nearby (slightly-perturbed) well-posed problem, whose resolution poses no difficulties (uniqueness, stability of the solution). The original solution is recovered only in the limit of vanishing regularization/perturbation parameter. The choice of the perturbation

term as well as the strength of the perturbation parameter is essential and constitutes the key point of the method. There is a rich literature on regularization techniques, we refer the interested reader to the references [7, 14, 16, 31].

Hence, an Asymptotic-Preserving scheme for an efficient resolution of the anisotropic transport equation (4.8) is based on the resolution of the following reformulated system

$$(MM)_\varepsilon^\sigma \quad \left\{ \begin{array}{l} \partial_t f^{\varepsilon,\sigma} + \mathbf{b}\cdot\nabla q^{\varepsilon,\sigma} = 0\,, \qquad \forall (t,\mathbf{x}) \in (0,T)\times\Omega\,, \\ \mathbf{b}\cdot\nabla f^{\varepsilon,\sigma} = \varepsilon\,\mathbf{b}\cdot\nabla q^{\varepsilon,\sigma} - \sigma\, q^{\varepsilon,\sigma}\,, \qquad \forall (t,\mathbf{x}) \in (0,T)\times\Omega\,, \end{array} \right. \tag{4.20}$$

with $\sigma > 0$ a small parameter to be fixed later on. This system is completed by an initial condition $f^{\varepsilon,\sigma}(0,\cdot) = f_{in}(\cdot)$ and adequate boundary conditions (*Hypothesis A*). Let us underline here the difference between (4.19) and (4.20). Both procedures are fixing the value of the auxiliary variable q on the field lines of $\mathbf{b}$ by imposing zero mean $\langle q\rangle = 0$. To see this in (4.20), it is enough to take the average $\langle\cdot\rangle$ of the second equation. However, while (4.19) is completely equivalent to the starting model (4.8), the system (4.20) introduces an error, as the supplementary term we introduced, $\sigma q^{\varepsilon,\sigma}$, is no more zero but contains also the non-zero fluctuation part of $q^{\varepsilon,\sigma}$, where the need to choose $\sigma > 0$ small enough. The big advantage of (4.20) with respect to (4.19) is that this time we have no more to discretize the average procedure $\langle\cdot\rangle$.

The ε-regularity of the system (4.20) allows now to pass directly to the $\varepsilon \to 0$ limit in (4.20) to get the corresponding limit model, *i.e.*

$$(MM)_0^\sigma \quad \left\{ \begin{array}{l} \partial_t f^{0,\sigma} + \mathbf{b}\cdot\nabla q^{0,\sigma} = 0\,, \\ \mathbf{b}\cdot\nabla f^{0,\sigma} + \sigma\, q^{0,\sigma} = 0\,. \end{array} \right. \tag{4.21}$$

Eliminating $q^{0,\sigma}$ from this system, yields the degenerate diffusion equation

$$\partial_t f^{0,\sigma} - \frac{1}{\sigma}\,\nabla\cdot\left[(\mathbf{b}\otimes\mathbf{b})\,\nabla f^{0,\sigma}\right] = 0\,, \tag{4.22}$$

which shows clearly what the regularization term is doing in the limit $\varepsilon \to 0$.

The numerical resolution of (4.8) is now based on a standard discretization of the reformulated problem (4.20). To be second order accurate, we decided to choose a DIRK-method for the time-discretization and the Arakawa scheme [1] for the discretization of the advection terms. This leads to the so-called (DAMM)-scheme (DIRK-Arakawa-Micro-Macro).

4.2 Numerical simulations of the Vlasov-Poisson problem

Let us now present some numerical results obtained with the (DAMM)-scheme for the resolution of the Vlasov-Poisson system

$$(VP)^\varepsilon \quad \left\{ \begin{array}{l} \partial_t f^\epsilon + \dfrac{1}{\epsilon}\,\{f^\epsilon, \Psi^\epsilon\} = 0\,, \quad \forall\,(t,x,v) \in (0,T)\times[0,L_x]\times[-L_v,L_v]\,, \\ -\partial_{xx}\varphi^\varepsilon(t,x) = 1 - n^\varepsilon(t,x)\,, \end{array} \right. \tag{4.23}$$

where we used the Poisson bracket (4.9) to simplify the notation and where furthermore $\Psi^\epsilon(t,x,v) := v^2/2 - \varphi^\epsilon(t,x)$ is the stream-function and $n^\varepsilon(t,x) := \int_{\mathbb{R}} f^\varepsilon(t,x,v)dv$ denotes the electron density. Due to the fact that this problem is non-linear (unlike the previous one), its study is a more delicate task. An iterative procedure shall cope with this nonlinearity.

The aim of the performed simulations was dual :

— validate the (DAMM)-scheme in a physical context and in the non-stiff case $\varepsilon = 1$, by comparing the obtained results with known analytic ones (as for ex. the growth rate of an instability) ;

— study the long-time asymptotics $\varepsilon \to 0$ of some specific physical phenomena, like the BKG-instabilities, for which no analytic result is available.

4.2.1 Numerical simulations in the non-stiff regime $\varepsilon = 1$

In order to validate our numerical procedure, we shall focus on the Landau damping as well as on the two-stream instability, for which analytic results are at hand. The Landau damping represents the exponential decrease of the electric field energy as a function of time [44, 51] and corresponds to an initial data of the form

$$f_{in}^{LD}(x,v) = \frac{1}{\sqrt{2\pi}}\left(1+\gamma\cos(kx)\right)e^{-v^2/2}\,, \quad k = 0.5\,,\ \ \gamma = 10^{-3}\,. \tag{4.24}$$

The two stream instability arises when two counter-streaming particle flows encounter each other leading to un unstable situation, reinforced by the nonlinearity of the medium. The nonlinear saturation of this instability leads to the concept of *nonlinear wave interactions* in the plasma. To simulate this kind of instability, one starts from an initial data of the form

$$f_{in}^{TS}(x,v) = \frac{1}{\sqrt{2\pi}}\left(1+\gamma\cos(kx)\right)\frac{1}{2}\left(e^{-(v-3)^2/2} + e^{-(v+3)^2/2}\right), \quad k = 0.2\,,\ \ \gamma = 10^{-3}\,. \tag{4.25}$$

On the left of Figure 4.1 we represent the evolution in time of the L^1-norm of the electric field $||E^\varepsilon(t,\cdot)||_1$ (in *log*-scale) obtained from the (DAMM)-scheme in the Landau damping context (4.24). So as to validate efficiently our (DAMM)-scheme, we plotted on the same Figure the corresponding evolution obtained via a reference spectral scheme for (4.23). The curves obtained from the two numerical schemes coincide perfectly. Moreover, we pay attention to the damping rate ω_i and the frequency of oscillations ω_p, which depend on the perturbation mode k. One sees that both schemes approach the analytic values (for $k = 0.5$), namely $\omega_i = -0.153$ and $\omega_p = 2\,\pi/T_p = 1.415$. On the left of Figure 4.1, we plot the evolution over time of the same quantity $||E^\varepsilon(t,\cdot)||_1$ (in *log*-scale) in the two-stream context (4.25). The analytic value of the growth rate for the electric field, *i.e.* $\omega_i(k = 0.2) = 0.2548$, is very close to the numerical value observed and the curves obtained via the two numerical schemes (DAMM and spectral) coincide. These two test-cases permitted to validate via physical arguments our (DAMM)-scheme in the $\varepsilon \sim 1$ regimes.

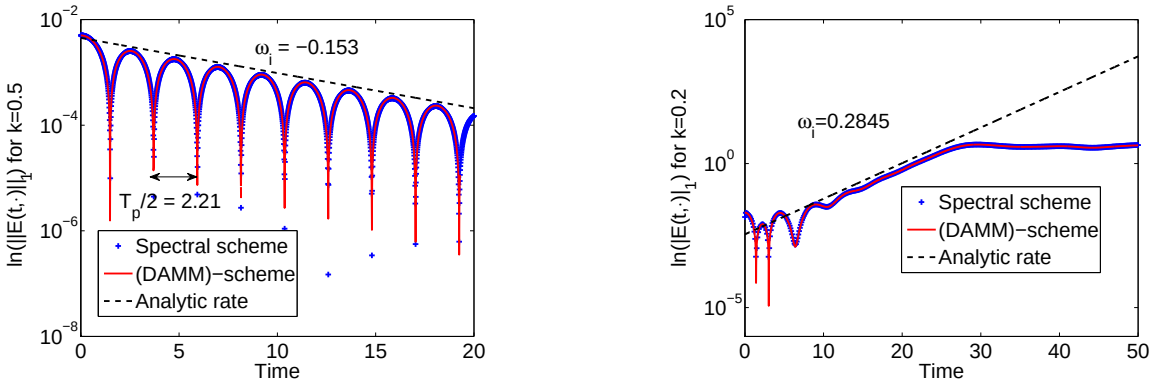

FIGURE 4.1: L^1-norm of the electric field (in log-scale) versus time . Left : Landau-damping test case (4.24). Right : Two-stream instability test case (4.25). $N_x = N_y = 256$, $\Delta t = 0.01$, $T = 20$, $\sigma = (\Delta x/L_x)^2$, $\varepsilon = 1$.

To conclude this section, we displayed on Figure 4.3 snapshots of the distribution function in phase-space at different times, with $\gamma = k = 0.3$ and Landau damping initial data (4.24). The filamentation of the distribution function is clearly visible, underlying the fact that the long-time convergence of the distribution function holds only in a weak sense.

4.2.2 Numerical simulations in the long-time regime $\epsilon \to 0$.

For the moment, the (DAMM)-scheme was validated via physical results, however its specific advantages, coming from the AP-property of the scheme, are not accentuated. This shall be the aim of this last section, where we show that the AP-property of the (DAMM)-scheme can be useful when an equilibrium is reached. Recall that in the case of the Vlasov-Poisson system (4.23), passing to $\varepsilon \to 0$ is equivalent to passing to $t \to \infty$. Thus, the (DAMM)-scheme seems suitable to study the long-time behavior of the non-linear two-stream instability. In this part, we modify the initial condition, taking

$$f_{in}^{BGK}(x,v) = \frac{1}{\sqrt{2\,\pi}}\, v^2 e^{-v^2/2}(1+\gamma\,\cos(k\,x))\,, \quad k = 0.5\,,\ \ \gamma = 5 * 10^{-2}\,. \tag{4.26}$$

Although no rigorous proof exists, the two-stream instability leads (in a certain weak sense) to a BGK (Bernstein-Greene-Kruskal) equilibrium after a growth phase. In Figure 4.2, the qualitative shape of such equilibrium is visible. We have plotted in panel (A) the obtained distribution function $f^0(t,x,v)$ via the (DAMM)-scheme, for $\varepsilon = 0$, $\Delta t = 0.1$ and after $n = 15$ times steps. Thanks to the AP-property of our (DAMM)-scheme, a BGK-equilibrium seems to be attained in very few time-steps, and with a very low numerical cost, without too much numerical pollution. One observes some sort of hole-like structure, the filamentations are smoothed out and the formation of a separatrix which connects the saddle points at $v = 0$ and $x = 0 = 4\,\pi$.

In order to confirm this BGK saturation, we shall check if the contours of the distribution function f^0 are aligned with the contours of the stream-function $\Psi^0 = v^2/2 - \varphi^0(x)$. Indeed, one expects that in the limit $\varepsilon \to 0$, f^0 becomes a function of Ψ^0, such that the Poisson bracket vanishes (see (4.23)). To put into evidence some sort of relation $f^0(\Psi^0)$ we plotted in panel (B) of Figure 4.2 f^0 versus Ψ^0 after some time-steps, and this for each point (x, v) in the phase space. A very clear curve is obtained which was compared with a fitting curve, in order to find out the $f^0(\Psi^0)$ functional relation. This last Figure confirms thus the affirmation of a $f^0(\Psi^0)$ dependence in the limit $\varepsilon \to 0$, and hence that we reached a saturated BGK-state.

To summarize, the (DAMM)-scheme permits, by passing to the limit $\varepsilon \to 0$, to obtain a BGK equilibrium with a low number of iterations, permitting to control the accumulation of the errors. This is an essential advantage, as compared to standard schemes.

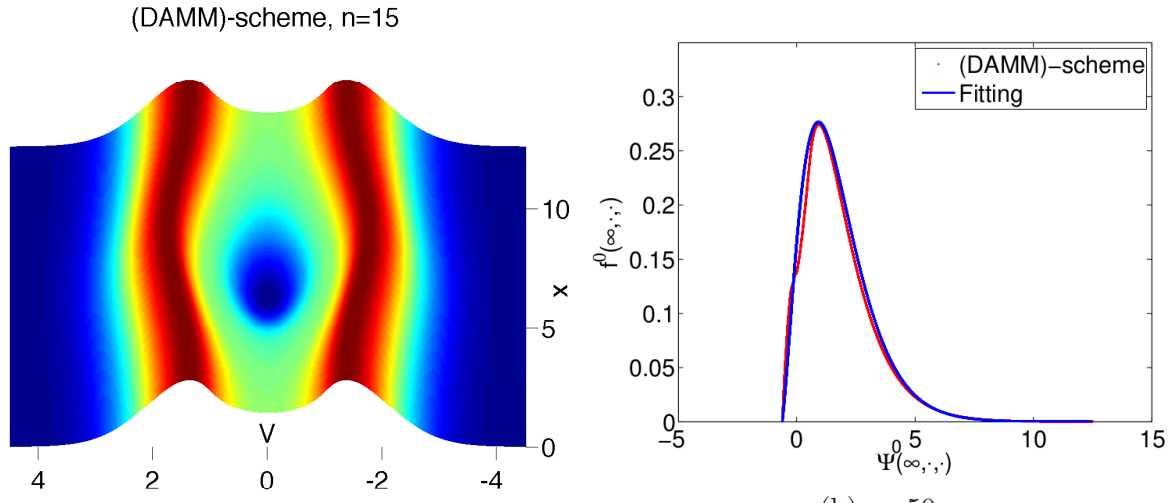

(a) n=15

(b) n=50

FIGURE 4.2: (Non-linear two-stream instability for $\varepsilon = 0$ and f_{in}^{BGK}) (a) Distribution function $f^0(t, x, v)$ obtained after $n = 15$ times steps. (b) $f^0(\Psi^0)$ relation obtained after $n = 15$ times steps. $N_x = N_y = 256$, $\Delta t = 0.1$, $\sigma = (\Delta x/L_x)^2$.

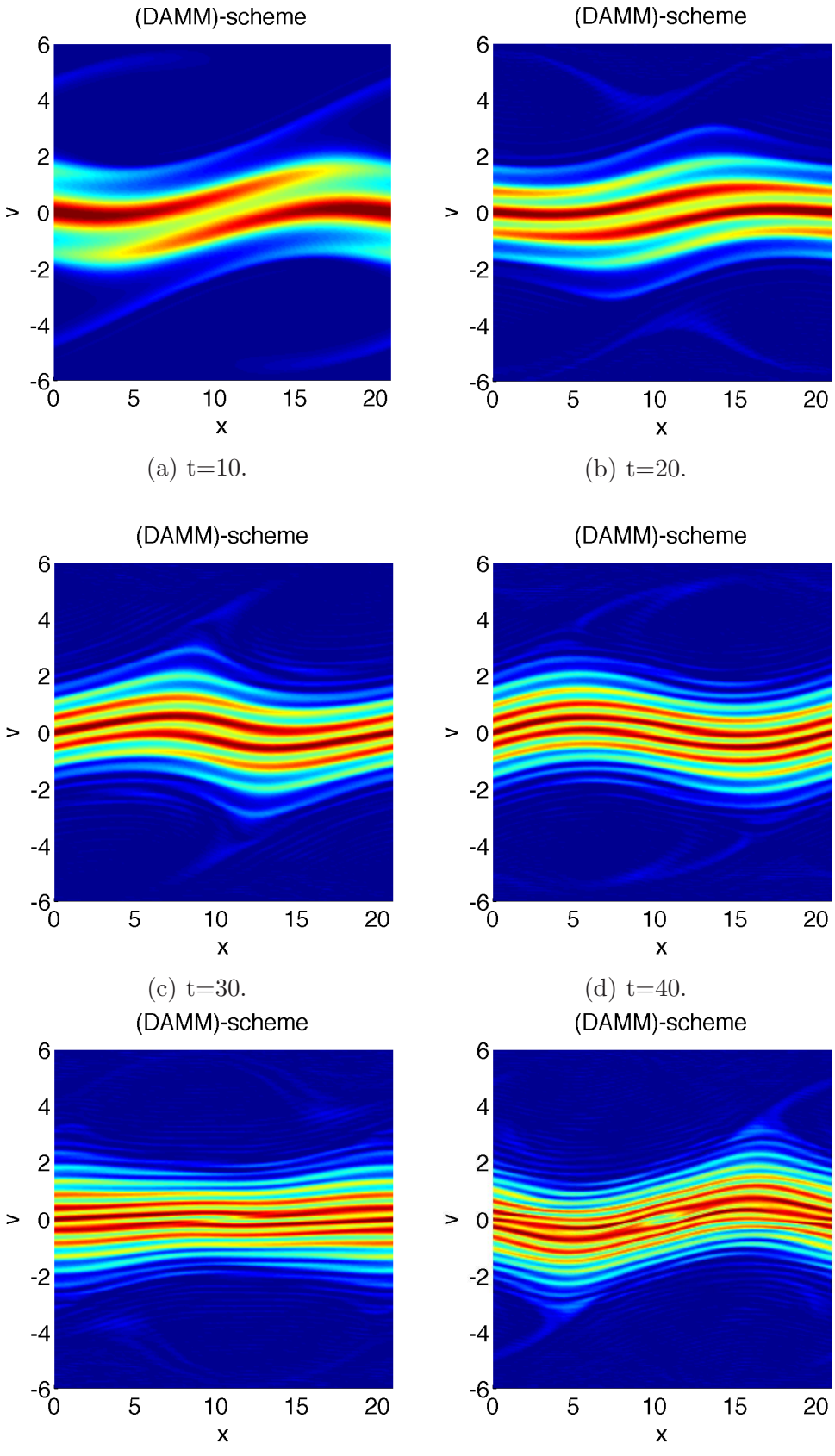

(a) t=10. (b) t=20.

(c) t=30. (d) t=40.

(e) t=50. (f) t=60.

FIGURE 4.3: (Strong Landau damping for $\epsilon = 1$) Snapshots of the distribution function $f^{\varepsilon}(t, x, v)$, at different times with $k = \gamma = 0.3$ and initial condition (4.24). $N_x = N_y = 256$, $\Delta t = 0.01$, $T = 60$, $\varepsilon = 1$ and $\sigma = (\Delta x / L_x)^2$.

Summary

We presented in this review some efficient numerical schemes developed to treat singularly perturbed problems. The main difficulty of singularly perturbed problems is the occurrence of stiff terms, induced by some small perturbation parameter $0 < \varepsilon \ll 1$. Hence, the solutions exhibit a multiscale character, which is difficult to capture numerically.

Some of the strategies introduced in this review for the construction of schemes preserving the asymptotic behaviour of the solutions in the limit $\varepsilon \to 0$ (called Asymptotic-Preserving schemes) are based on a detailed mathematical study of the dominant operator, the identification of the Limit model as $\varepsilon \to 0$ and the decomposition of the unknown in a macroscopic part (belonging to the kernel of the dominant operator) and a microscopic part. These two parts satisfy a coupled system of equations, equivalent to the initial singularly perturbed system. The advantage of the Micro-Macro system is that it leads automatically to the Limit model, when the perturbation parameter ε tends to zero. We would like to underline here that the construction of AP-schemes is not unique, and several other AP-strategies are presented in literature, for example based on a combination of splitting, penalization (see Chapter 3), exponential, filtering methods. The Micro-Macro approach presented in this review is a rather elegant and systematic strategy, allowing also for a rigorous mathematical study.

After the obtention of the Micro-Macro coupled system, one has to take care when discretizing this system in order not to destroy the AP-properties with a non-adapted discretization. Several numerical tests have been also presented in this review to illustrate the efficiency of the developed AP-schemes. In particular these schemes are shown to be uniformly stable (in ε) along the transition from the initial problem (microscopic level) to the Limit problem (macroscopic level). This property is very important in practical applications, where the perturbation parameter can vary considerably within the study domain. In other words, the AP-schemes are able to approximate uniformly accurate the solutions in both regimes, microscopic as well as macroscopic, and this on ε-independent grids, which have not to be adapted to the anisotropy direction.

The Asymptotic-Preserving techniques presented in this review can be applied to other singularly perturbed problems, coming from physics, biology, chemistry, economy *etc.* But each time, one has to study independently the occurring dominant operator and construct an adapted AP-scheme for the special problem. No general AP-methodology can be proposed, valid for all problems.

Bibliographie

[1] A. Arakawa, Computational design for long-term numerical integration of the equations of fluid motion : two dimensional incompressible flow, *Journal of Computational Physics*, **135** (1966), 119–143.

[2] D. Aronson, *The porous medium equation*, A. Fasano, M. Primicerio (Eds.), Nonlinear Diffusion Problems, Lecture Notes in Mathematics **1224** (1986), 1-46.

[3] A. Arseneev, *Global existence of a weak solution of the Vlasov system of equations*, U.R.S.S. Comp. Math. Phys. **15** (1975), 131–143.

[4] C. Bardos, P. Degond, *Global existence for the Vlasov-Poisson equation in three space variables with small initial data*, Ann. Inst. H. Poincaré, Anal. non linéaire **2** (1985), 101–118.

[5] R. Belaouar, N. Crouseilles, P. Degond, E. Sonnendrücker, *An asymptotically stable semi-lagrangian scheme in the quasi-neutral limit*, Journal of Scientific Computing **41** (2009), 341–365.

[6] N. Ben Abdallah, P. Degond, *On a hierarchy of macroscopic models for semiconductors*, J. Math. Phys. **37** (1996), 3306–3333.

[7] P.B Bochev and R. B Lehoucq, Regularization and stabilization of discrete saddle-point variational problems, *Electronic Transactions on Numerical Analysis*, **22** (2006), 97–113.

[8] M. Bostan, *The Vlasov-Maxwell system with strong initial magnetic field. Guiding-center approximation*, SIAM J. Multiscale Model. Simul. **6** (2007), no. 3, 1026-1058.

[9] M. Bostan, The Vlasov-Poisson system with strong external magnetic field. Finite Larmor radius regime, Asymptot. Anal. **61** (2009), 91-123.

[10] M. Bostan, Transport equations with disparate advection fields. Application to the gyrokinetic models in plasma physics, *SIAM J. Sci. Comp.*, **31** (2008), 334–368.

[11] M. Bostan, Transport equations with singular coefficients. Application to the gyrokinetic models in plasma physics, research report INRIA, hal :inria-00232800, submitted 2009.

[12] M. Bostan, Gyrokinetic Vlasov equation in three dimensional setting. Second order approximation, IAM J. Multiscale Model. Simul., **8** (2010), no. 5, 1923-1957.

[13] Y. Brenier, *Convergence of the Vlasov-Poisson system to the incompressible Euler equations*, Comm. Partial Differential Equations **25** (2000), 737–754.

[14] C. Brezinski, M. Redivo-Zaglia, G. Rodriguez and S. Seatzu, Multi-parameter regularization techniques for ill-conditioned linear systems, *Numer. Math.*, **94** (2003), 203–228.

[15] S. Brull, P. Degond, F. Deluzet, A. Mouton, *Asymptotic-Preserving scheme for a bi-fluid Euler-Lorentz model*, Kinetic and Related Models **4** (2011), 991 - 1023.

[16] D. Calvetti, S. Morigi, L. Reichel and F. Sgallari, Tikhonov regularization and the L-curve for large discrete ill-posed problems, *J. Comput. Appl. Math.*, **123** (2000), 423–446.

[17] F.F Chen, *Plasma Physics and Controlled Fusion*, Springer, New-York, 2006.

[18] F. Cordier, P. Degond, A. Kumbaro, *An Asymptotic-Preserving all-speed scheme for the Euler and Navier-Stokes equations*, Journal of Computational Physics.

[19] P. Crispel, P. Degond, M-H. Vignal, *An asymptotic preserving scheme for the two-fluid Euler-Poisson model in the quasineutral limit*, J. Comp. Phys. **223** (2007), 208-234.

[20] N. Crouseilles, M. Lemou, *An asymptotic preserving scheme based on a micro-macro decomposition for collisional Vlasov equations : diffusion and high-field scaling limits* , KRM **4** (2011), 441–477.

[21] F. Coron, B. Perthame, *Numerical passage from kinetic to fluid equations*, SIAM J. Numer. Anal. **28** (1991), 26–42.

[22] P. Degond *Macroscopic limits of the Boltzmann equation : a review*, Modeling and Computational Methods for Kinetic Equations, Springer Science+Business Media New York 2004.

[23] P. Degond, F. Deluzet, L. Navoret, A-B. Sun, M-H.Vignal *Asymptotic-Preserving Particle-In-Cell method for the Vlasov-Poisson system near quasineutrality*, J. Comput. Phys. **229** (2010), 5630–5652.

[24] P. Degond, F. Deluzet, A. Sangam, M-H. Vignal, *An asymptotic preserving scheme for the Euler equations in a strong magnetic field*, J. Comput. Phys. **228** (2009), 3540-3558.

[25] P. Degond, J-G. Liu, M-H. Vignal, *Analysis of an asymptotic preserving scheme for the Euler-Poison system in the quasineutral limit*, SIAM J. Numer. Anal. **46** (2008), 1298-1322.

[26] P. Degond, M. Tang, *All speed scheme for the low mach number limit of the Isentropic Euler equation*, Communications in Computational Physics, **10** (2011), 1-31.

[27] G. Dimarco, L. Pareschi, "Exponential methods for kinetic equations", SIAM J. Num. Anal. **49** (2011), 2057-2077.

[28] G. Dimarco, L. Pareschi, "High order asymptotic-preserving schemes for the Boltzmann equation", Comptes Rendus Mathematique **350** (2012), 481-486.

[29] R. J. DiPerna, P.-L. Lions, *Global weak solutions of the Vlasov-Maxwell system*, Comm. Pure Appl. Math. XVII (1989), 729–757.

[30] W. E *Principles of multiscale modeling*, Cambridge university press, 2011.

[31] H. W. Engl, M. Hanke, and A. Neubauer, *Regularization of Inverse Problems*, Kluwer Academic Publishers, Netherlands, 1996.

[32] F. Filbet, S. Jin, "A class of asymptotic preserving schemes for kinetic equations and related problems with stiff sources", J. Comp. Physics **229** (2010), no. 20, .

[33] F. Filbet, S. Jin, "An Asymptotic Preserving Scheme for the ES-BGK model of the Boltzmann equation", J. Sci. Computing **46** (2011), no. 2, 204-224.

Homogenization of the Vlasov equation and of the Vlasov-Poisson system with strong external magnetic field, Asymptotic Anal. **18** (1998), 193-213.

[34] F. Golse, L. Saint-Raymond, *The Vlasov-Poisson system with strong magnetic field in quasineutral regime*, Math. Models and Meth. in Appl. Sci. **13** (2003), 661-714).

[35] F. Golse, L. Saint-Raymond, *The Vlasov-Poisson system with strong magnetic field*, J. Math. Pures et Appl. **78** (1999), 791-817.

[36] E. Grenier, *Limite quasi-neutre en dimension 1*, Journées Équations aux dérivées partielles (1999), 1-8.

[37] R.D. Hazeltine and J.D. Meiss, *Plasma Confinement*, Dover Publications, Inc. Mineola, New-York, 2003.

[38] M. H. Holmes, *Introduction to perturbation methods*, Springer-Verlag, New York, 1995.

[39] E. Horst, R. Hunze, *Weak solutions of the initial value problem for the unmodied nonlinear Vlasov equation*, Math. Meth. Appl. Sci. **6** (1984), 262–279.

[40] S. Jin *Efficient Asymptotic-Preserving (AP) schemes for some multiscale kinetic equations*, SIAM J. Sci. Comp. **21** (1999), 441–454.

[41] S.Jin, L.Pareschi, G.Toscani, *Diffusive relaxation schemes for multiscale discrete-velocity kinetic equations*, SIAM J. Numerical Analysis **35** (1998), no. 6, 2405–2439.

[42] A. Klar, *An Asymptotic Induced Scheme for Nonstationary Transport Equations in the Diffusive Limit*, SIAM J. Num. Anal. **35** (1998), no. 3, 1073–1094.

[43] A. Klar, *Asymptotic Induced Domain Decomposition Methods for Kinetic and Drift Diffusion Semiconductor Equations*, SIAM J. Sci. Comp. **19** (1998), no. 6, 2032–2050.

[44] L. Landau, On the vibration of the electronic plasma. *English translation in J. Phys. (USSR)*, **10** (1946), 25.

[45] C. Le Bris, *Systèmes multi-échelles. Modélisation et simulation*, Springer-Verlag, Berlin Heidelberg, 2005.

[46] M. Lemou, F. Méhats, *Micro-macro schemes for kinetic equations including boundary layers.*

[47] M. Lemou, L. Mieussens, "A new asymptotic preserving scheme based on micro-macro formulation for linear kinetic equations in the diffusion limit", SIAM J. Sci. Comput. **31** (2008), no. 1, 334–368.

[48] P.-L. Lions, B. Perthame, *Propagation of moments and regularity for the 3- dimensional Vlasov-Poisson system*, Invent. Math. **105** (1991), 415–430.

[49] J.-G. Liu, L. Mieussens, *Analysis of an asymptotic preserving scheme for linear kinetic equations in the diffusion limit*, SIAM J. Numer. Anal. **48** (2010), no. 4, 14741491.

[50] A. Lozinski, J. Narski, C. Negulescu, *Highly anisotropic temperature balance equation and its asymptotic-preserving resolution*, M2AN (Mathematical Modelling and Numerical Analysis) **48** (2014) 1701–1724.

[51] C.Villani and C. Mouhot, On Landau damping, *Acta Math.*, **207** (2011), 29–201.

[52] A. J. Majda and A. L Bertozzi, *Vorticity and Incompressible Flow*, Cambridge University Press, United Kingdom, 2002.

[53] A. Mentrelli, C. Negulescu, *Asymptotic-Preserving scheme for highly anisotropic non-linear diffusion equations*, Journal of Comp. Phys.

[54] J. Narski, M. Ottaviani, *Asymptotic-Preserving scheme in a magnetic island context*, in preparation.

[55] K. Pfaffelmoser, *Global classical solutions of the Vlasov-Poisson system in three dimensions for general initial data*, J. Differential Equations **95** (1992), 281–303.

[56] F. Poupaud, *Diffusion approximation of the linear semiconductor Boltzmann equation : analysis of boundary layers*, Asymptotic Analysis **4** (1991), 293–317.

[57] R. J. Goldston, P.H. Rutherford, *Plasma Physics*, Taylor & Francis Group, Philadelphia, 1995.

[58] J. Schaeffer, *Global existence of smooth solutions to the Vlasov-Poisson system in three dimensions*, Comm. Partial Differential Equations **16** (1991), 1313–1335.

[59] J. Vázquez, *The porous medium equation : mathematical theory*, Oxford University Press, USA, 2007.